

Exemestane plus everolimus and palbociclib in metastatic breast cancer: clinical response and genomic/transcriptomic determinants of resistance in a phase I/II trial

Received: 9 October 2022

Accepted: 2 February 2024

Published online: 19 March 2024

 Check for updates

A list of authors and their affiliations appears at the end of the paper

The landscape of cyclin-dependent kinase 4/6 inhibitor (CDK4/6i) resistance is still being elucidated and the optimal subsequent therapy to overcome resistance remains uncertain. Here we present the final results of a phase Ib/IIa, open-label trial (NCT02871791) of exemestane plus everolimus and palbociclib for CDK4/6i-resistant metastatic breast cancer. The primary objective of phase Ib was to evaluate safety and tolerability and determine the maximum tolerated dose/recommended phase II dose (100 mg palbociclib, 5 mg everolimus, 25 mg exemestane). The primary objective of phase IIa was to determine the clinical benefit rate (18.8%, $n = 6/32$), which did not meet the predefined endpoint (65%). Secondary objectives included pharmacokinetic profiling (phase Ib), objective response rate, disease control rate, duration of response, and progression free survival (phase IIa), and correlative multi-omics analysis to investigate biomarkers of resistance to CDK4/6i. All participants were female. Multi-omics data from the phase IIa patients ($n = 24$ tumor/17 blood biopsy exomes; $n = 27$ tumor transcriptomes) showed potential mechanisms of resistance (convergent evolution of HER2 activation, $BRAF^{V600E}$), identified joint genomic/transcriptomic resistance features ($ESR1$ mutations, high estrogen receptor pathway activity, and a Luminal A/B subtype; $ERBB2/BRAF$ mutations, high RTK/MAPK pathway activity, and a HER2-E subtype), and provided hypothesis-generating results suggesting that mTOR pathway activation correlates with response to the trial's therapy. Our results illustrate how genome and transcriptome sequencing may help better identify patients likely to respond to CDK4/6i therapies.

The combination of cyclin-dependent kinase 4/6 inhibitors (CDK4/6i) (palbociclib, ribociclib, abemaciclib) and endocrine therapy has become standard of care for the treatment of patients with hormone receptor-positive (HR+), human epidermal growth factor receptor 2-negative (HER2-) metastatic breast cancer (MBC). However, some patients do not respond at all to CDK4/6i therapy (intrinsic resistance)

while other patients initially respond but eventually become refractory to therapy (acquired resistance), which results in disease progression.

Multiple studies in the last few years have started to reveal the genomic landscape of resistance to CDK4/6 inhibitors¹. One major class of resistance mechanisms that have been observed in the clinical setting are alterations that activate the cell cycle pathway, namely, loss-

 e-mail: Nikhil_Wagle@dfci.harvard.edu

of-function alterations in *RBI*^{2–5} and high cyclin E1 (*CCNE1*) mRNA expression⁶. Other notable potential resistance mechanisms in the cell cycle pathway are amplifications of *AURKA*⁵ and *CDK6* overexpression^{7–9}.

In addition to the cell cycle pathway, multiple oncogenic pathways have been associated with resistance to CDK4/6 inhibitors in the clinical setting. In the estrogen receptor (ER) pathway, low ER expression^{5,6} and basal molecular subtype¹⁰ have been associated with a lack of response to CDK4/6 inhibitors. Loss-of-function of *FAT1*, which activates the Hippo pathway and results in an increase in *CDK6* expression, has been associated with poor response to CDK4/6i therapy⁴. Oncogenic alterations in the receptor tyrosine kinase (RTK) (*FGFR1*, *FGFR2*, *ERBB2*), MAPK (*KRAS*, *HRAS*, *NRAS*), and PI3K/AKT/mTOR (*AKT1*, *PTEN*) pathways, all of which are upstream of the cell cycle pathway, have been found to be enriched in patient samples that are resistant to CDK4/6 inhibitors and to cause resistance in pre-clinical models^{5,11–15}.

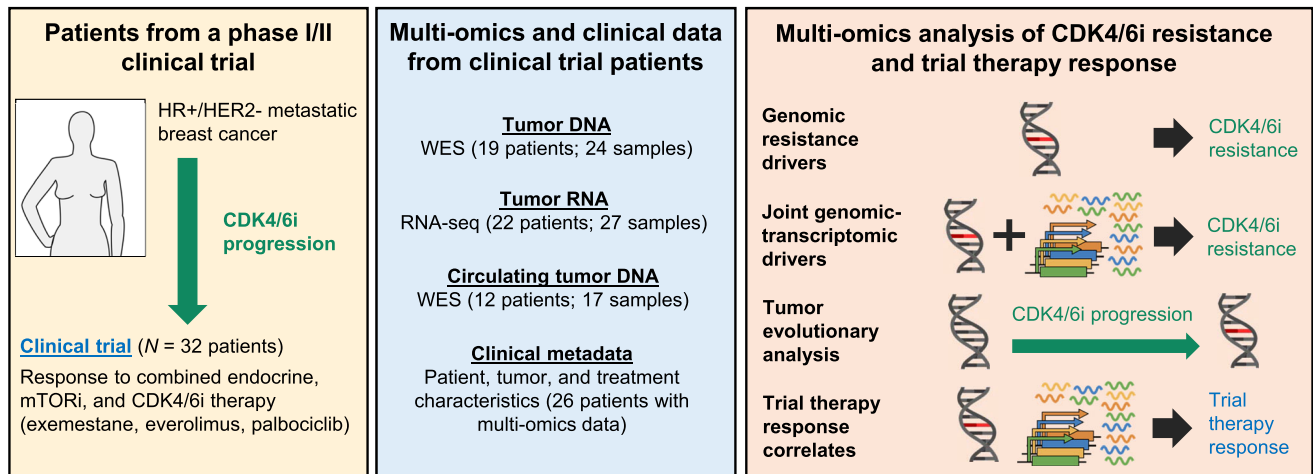
Despite the variety of genomic resistance mechanisms and pathways identified by this recent work, the complete landscape of CDK4/6i resistance is still being elucidated. In particular, the transcriptomic landscape has remained mostly unexplored.

Oncogenic alterations in the RTK, MAPK, and PI3K/AKT/mTOR pathway have also been found to confer resistance to endocrine therapies^{11,12,16–18}. This is analogous to the role that alterations in these pathways play in CDK4/6 therapy, since the canonical resistance mechanisms to endocrine therapy are alterations that directly affect the ER (primarily activating *ESR1* mutations)^{16–18}.

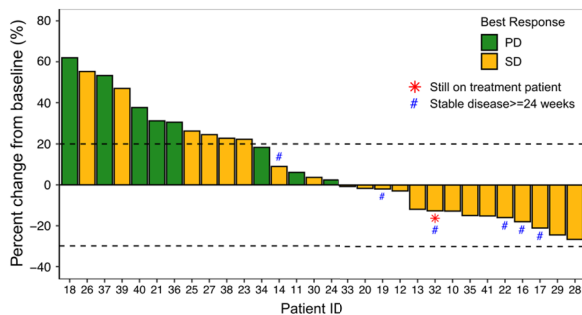
Given that RTK, MAPK, and PI3K/AKT/mTOR oncogenic alterations drive resistance to both endocrine therapy and CDK4/6i, targeting these pathways might overcome resistance. For endocrine-resistant MBC, the BOLERO-2 phase III trial found that the combination of exemestane (an aromatase inhibitor) and everolimus (an mTOR inhibitor) resulted in a longer progression-free survival than exemestane alone¹⁹. Whether an analogous result holds for the combination of CDK4/6i, endocrine therapy, and everolimus or other PI3K/AKT/mTOR targeted therapy is still an open question for CDK4/6i-resistant MBC.

Here we report the final results from a phase I/II clinical trial evaluating the safety and efficacy of exemestane plus everolimus and palbociclib, triplet therapy in patients with CDK4/6i-resistant and endocrine-resistant HR+ MBC (NCT02871791). By leveraging multi-omics data from patients that participated in this trial—whole-exome sequencing (WES) and RNA sequencing (RNA-seq) of tumor biopsies and circulating tumor DNA (ctDNA), accompanied by comprehensive clinical data—we performed an integrated analysis of the molecular correlates of both the landscape of resistance to initial CDK4/6 inhibitors and the response to triplet therapy (Fig. 1A). Our analysis identifies genomic alterations in resistance genes (*ESR1*, *ERBB2*, *AKT1*, *RBI*, *BRAF*), genomic/transcriptomic resistance features (concurrent HER2-enriched molecular subtype and RTK/MAPK oncogenic mutations, concurrent ER pathway activity and *ESR1* oncogenic mutations), evidence of convergent evolution of *ERBB2* activation following progression on CDK4/6i therapy, and indicators that the mTOR pathway activity is associated with response to triplet therapy. In this work, we take an important step towards elucidating the complete landscape of

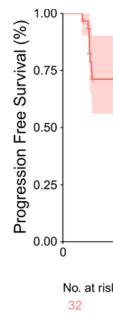
A



B



C



D

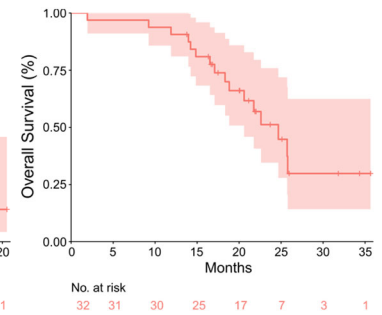


Fig. 1 | Methodological overview of this work and plots for the phase II portion of the clinical trial. A Graphical methodological overview. **B** Waterfall plot of best percentage change from baseline of tumor lesions. Patients 15 and 31, who stopped treatment before tumor response could be evaluated, were excluded from this plot.

C Progression-free survival (PFS) Kaplan–Meier curve. The median PFS is 3.94 months (95% confidence interval (CI): 3.68–9.63). **D** Overall survival (OS) Kaplan–Meier curve. The median OS is 24.7 months (95% CI: 20.6 – N/A). *n* = 32 patients were included in the phase II portion of the trial.

resistance to CDK4/6i in HR + /HER2 – MBC and highlight how multi-omics data may better identify factors that determine response to CDK4/6i therapy (Fig. 1).

Results

Patients received limited clinical benefit from triplet therapy

Patients participated in an investigator initiated phase Ib/IIa, open-label clinical trial (NCT02871791) evaluating the safety and efficacy of triplet therapy: palbociclib (a CDK4/6 inhibitor) + everolimus (mTOR inhibitor) + exemestane (steroidal aromatase inhibitor). Eligible patients had been diagnosed with HR + /HER2 – MBC and had progressed on a prior CDK4/6i and a prior endocrine therapy (a non-steroidal aromatase inhibitor).

Phase Ib MTD/RP2D. A total of 9 patients were recruited into the phase Ib portion of the study between September 12, 2016 and March 27, 2017. All study participants were female. At the starting dose of palbociclib (100 mg), 1 out of 3 patients experienced a DLT (grade 3 neutropenia and grade 2 mucositis). Subsequently, 3 additional patients were initiated at 100 mg, and none experienced a DLT. Palbociclib was increased to 125 mg, and all 3 patients had a DLT (grade 3 neutropenia). Thus, 100 mg palbociclib was declared the MTD. The RP2D for phase IIa was 100 mg palbociclib + 5 mg everolimus + 25 mg exemestane²⁰.

PK profile. The 9 patients in the phase Ib portion of the study were included in the PK analysis (Supplementary Data 1). The mean steady state PK parameters for palbociclib, everolimus, and exemestane was found to be consistent with historical data for each drug given as a single agent, and thus, we did not find evidence of significant PK drug interactions when the three drugs are given concurrently.

Phase IIa Patient characteristics. A total of 32 patients were recruited into the phase IIa portion of the study between May 26, 2017 and June 26, 2019. Patient disposition at the time of data cutoff (Jan 3, 2021) is reported in Supplementary Table 1. All study participants were female, with a median age (range) of 55.5 years (36–73). Most of the participants were initially diagnosed with stage I–III breast cancer and had a disease-free interval longer than two years. However, a substantial percentage of patients ($n=10/32$, 31.2%) had been diagnosed with de novo metastatic breast cancer. Bone ($n=28/32$, 87.5%), liver ($n=26/32$, 81.3%) and CNS + lung + liver ($n=27/32$, 84.4%) were the most common sites of metastases (Supplementary Table 2).

Approximately one-third of patients had received one line of prior chemotherapy in the metastatic setting ($n=12/32$, 37.5%); the remainder had received no prior chemotherapy ($n=20/32$, 62.5%). Among patients who had received prior chemotherapy in the metastatic setting, capecitabine was the most commonly used agent ($n=7/32$, 21.9%). Almost all patients had received at least one prior line of endocrine therapy ($n=31/32$, 96.9%), and over half had received 2 or more prior lines ($n=17/32$, 53.1%). All but 2 patients had received palbociclib ($n=30/32$, 93.8%) and the remaining 2 patients had received abemaciclib ($n=2/32$, 6.3%).

Efficacy. With a median follow-up (interquartile range) of 23.7 months (20.1–31.8 months), 6 patients had stable disease (SD) ≥ 24 weeks ($n=6/32$, 18.8%), 18 patients had SD ≥ 12 weeks ($n=18/32$, 56.3%), and 8 patients had progressive disease (PD) ($n=8/32$, 25.0%) as best response (Fig. 1B, Supplementary Table 3). The clinical benefit rate (CBR, CR + PR + SD ≥ 24 weeks) was 18.8%, which was below the pre-specified efficacy endpoint of CBR $\geq 65\%$. Median progression-free survival (PFS) was 3.94 months (95% CI: 3.68–9.63) (Fig. 1C) and median overall survival (OS) was 24.7 months (95% CI: 20.6 - not reached) (Fig. 1D). For the patients that derived and did not derive clinical benefit, PFS was 9.63 months (95% CI: 8.44 - not reached) and

3.78 months (95% CI: 2.00 - 4.70), and OS was 22.6 months (95% CI 16.5 - not reached) and 24.7 months (95% CI: 18.80 - not reached), respectively. Median duration of response (DOR) was 5.42 months (95%CI: 3.74–9.62) and disease control rate (DCR, CR + PR + SD ≥ 12 weeks) was 56.3%.

Safety. The most common all-grade adverse events related to study treatment were neutropenia ($n=29/32$, 90.6%), oral mucositis ($n=17/32$, 53.1%), thrombocytopenia ($n=9/32$, 28.1%), and fatigue ($n=8/32$, 25.0%). A total of 25 patients ($n=25/32$, 78.1%) experienced neutropenia of grade 3 or higher (Supplementary Table 4). Most treatment-related adverse events were likely caused by palbociclib and/or everolimus in this combination regimen (Supplementary Table 4).

25 patients ($n=25/32$, 78.1%) had a dose hold of palbociclib due to toxicity, and 16 patients ($n=16/32$, 50.0%) had at least one dose reduction. Furthermore, 22 patients ($n=22/32$, 68.8%) had a dose hold of everolimus, and 13 ($n=13/32$, 40.6%) had at least one dose reduction due to toxicity. Exemestane was held in 2 patients ($n=2/32$, 6.3%) due to toxicity, and no participants required a dose reduction of exemestane (Supplementary Table 5). Patient-level clinical characteristics are in Supplementary Data 3.

Whole exome and transcriptome sequencing of baseline tumor and ctDNA revealed potential resistance mechanisms to CDK4/6 inhibitors and endocrine therapy

As part of the secondary objective of the clinical trial to investigate biomarkers of resistance to CDK4/6i through a correlative multi-omics analysis, we generated WES and RNA-seq data from tumor biopsies and ctDNA samples from patients who participated in the phase II portion (Fig. 2A, Supplementary Data 4, Supplementary Data 5). We collected a research tumor biopsy and blood sample at baseline (after progression on the prior CDK4/6 inhibitor but before initiation of triplet therapy) and additional serial blood samples while on the trial. Additionally, when possible, we acquired archival tumor biopsies that preceded the patient's initial exposure to a CDK4/6i to serve as a CDK4/6i-naive sample. Given the exploratory nature of this study and our limited sample size, significance tests in our analyses were not corrected for multiple comparisons.

For the baseline tumor biopsies (annotated as T1), WES or RNA-seq was successfully performed and passed quality-control for 18 samples each, with 14 samples having both WES and RNA-seq data (Fig. 2A). WES was successfully performed and passed quality-control for 17 ctDNA samples (12 at baseline, annotated as BBI, and 5 while on therapy, annotated as BBn) from 12 patients, with 11 patients having WES from both a baseline tumor and ctDNA sample. For the pre-CDK4/6i tumor biopsies (annotated as A1), WES or RNA-seq was successfully performed and passed quality-control for 6 and 9 samples, respectively, with 5 patients having WES from both a pre-CDK4/6i and a baseline biopsy. The complete dataset consisted of data from 26 patients: germline-matched WES from 24 tumor samples (19 patients) and 17 ctDNA samples (12 patients), and RNA-seq from 27 tumor samples (22 pts) (Fig. 2A).

We first focused on the genomic landscape (WES) of the baseline tumor and blood biopsies (18 T1's, 12 BBI's, $n=19$ pts with either a T1 or BBI) (Fig. 2A, Supplementary Data 4, Supplementary Data 5). We identified genomic alterations spanning the spectrum of known genes and pathways previously identified to confer resistance to CDK4/6 inhibitors in 58% ($n=11/19$) of patients^{3–5,7,13} and to endocrine therapy in 74% ($n=14/19$) of patients^{11,12,16–18}. These pathways, genes, and alterations include: *PTEN* bi-allelic inactivations ($n=1/19$, 5% of patients) and *AKT1* activating mutations ($n=4/19$, 21%) in the PI3K/AKT/mTOR pathway; *NFI* bi-allelic inactivations (1/19, 5%) in the MAPK pathway; *ERBB2* activating mutations ($n=2/19$, 11%), *FGFR1* activating mutations ($n=1/19$, 5%) or high amplifications (5/19, 26%), and *FGFR2*

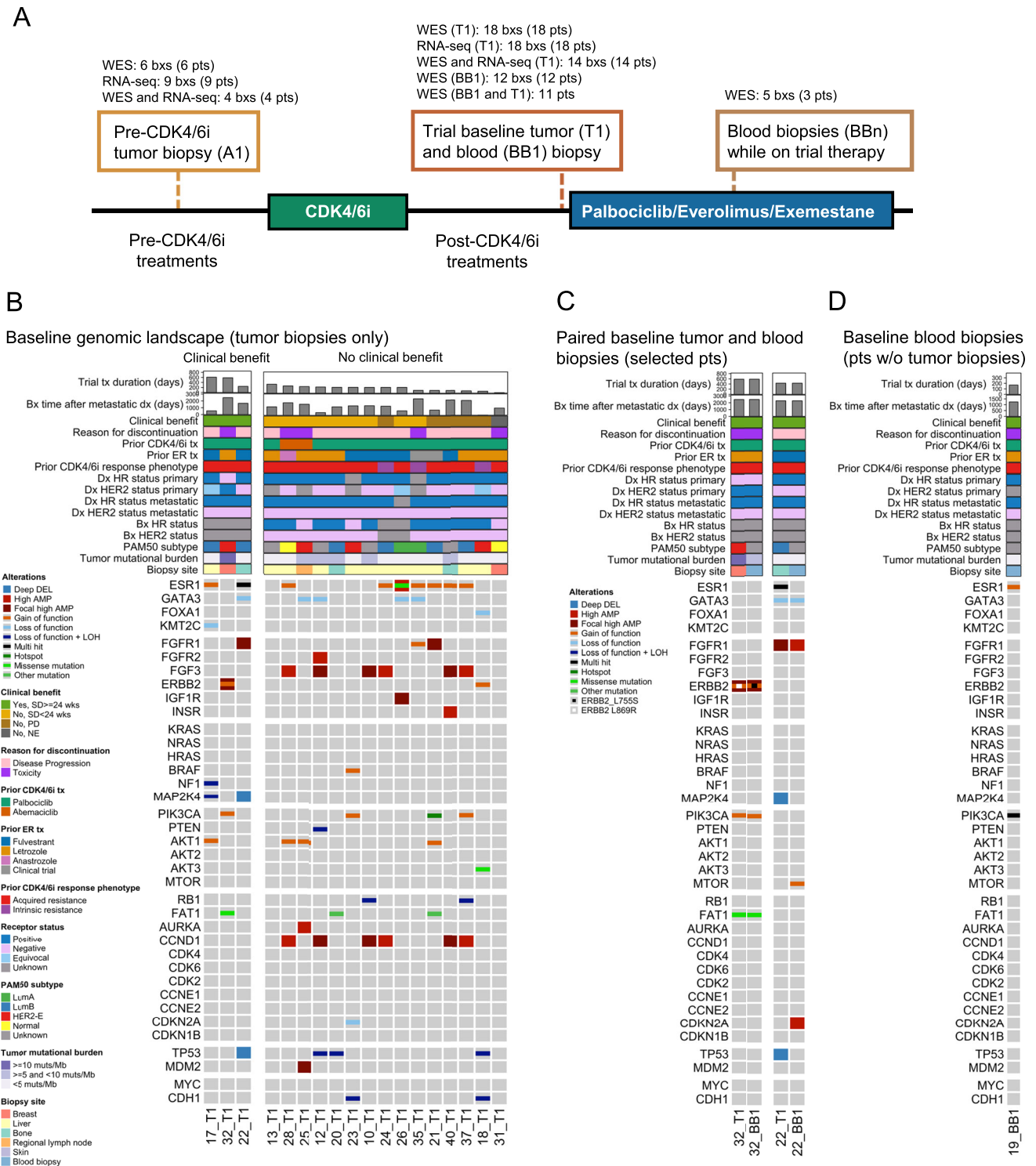


Fig. 2 | Genomic landscape of resistance to CDK4/6 inhibitors in clinical trial baseline biopsies. The genomic landscape recapitulates known driver genes and pathways of CDK4/6i resistance and putative driver genes and mutations (*BRAF*^{V600E}, *MTOR*^{T197R}, *PIK3CA*^{E545K, G1007R}). **A** Cohort of tumor and blood biopsies used for multi-omics analysis and their timing. Patients received triplet therapy (palbociclib + everolimus + exemestane) as part of the clinical trial, and had progressed on a prior CDK4/6i and a prior endocrine therapy. **B–D** Comutation plots (CoMut) representing the genomic landscape of baseline tumor and blood biopsies from the clinical trial. All baseline tumor biopsies are shown in **(B)** ($n = 18$ samples from $n = 18$ patients); paired baseline tumor and blood biopsies from patients with distinct co-existing tumor lineages are shown in **(C)** ($n = 4$ samples from $n = 2$ patients); baseline blood biopsies from patients with no paired tumor biopsy are shown in **(D)** ($n = 1$ sample from $n = 1$ patient). In each panel, biopsies are ordered by

treatment duration on triplet therapy. Copy-number alterations and nonsynonymous mutations from selected genes (including all from Wander et al.)⁵ are shown. Genes are arranged based on their pathway and include all genes with 2 or more known oncogenic mutations in the cohort. Clinical parameters shown include trial treatment duration, clinical benefit and best response by RECIST 1.1, reason for discontinuation of treatment, prior CDK4/6i treatment information (CDK4/6i received, anti-estrogen agent used in combination, phenotype based on prior CDK4/6i response), receptor status (biopsy-level, at primary diagnosis, and at metastatic diagnosis), timing of biopsy relative to metastatic diagnosis, and biopsy site. Research-based PAM50 subtype (when RNA-seq data is available) and tumor mutational burden of each biopsy are also shown. Source data are provided as a Source Data file.

high amplifications ($n = 1/19$, 5%) in RTKs; *RBI* bi-allelic inactivations ($n = 2/19$, 11%) and *AURKA* high amplifications ($n = 1/19$, 5%) in cell cycle genes; activating mutations in *ESR1* ($n = 9/19$, 47%) in the ER pathway. In addition to these genomic alterations, we also observed loss of ER expression (as measured by immunohistochemistry (IHC)) in baseline tumor samples ($n = 3/19$, 16%), which we refer to as “loss of ER expression” because these patients were previously diagnosed with ER + /HER2- metastatic breast cancer.

In addition to the alterations in these known resistance genes and pathways, we identified three potential resistance mechanisms in genes belonging to these pathways: an activating *BRAF*^{V600E} mutation (MAPK) (in patient 23, Fig. 2B), an activating *MTOR*^{T197R} mutation (PI3K/AKT/MTOR) (in patient 22, Fig. 2C), and activating double *PIK3CA*^{E545K,G1007R} mutation (PI3K/AKT/mTOR) (in patient 19, Fig. 2D). All of these mutations were clonal in the baseline biopsy in which they were identified. The activating *BRAF* mutation was not detected in the pre-CDK4/6 inhibitor biopsy, and thus was acquired/enriched following the treatment with the initial CDK4/6 inhibitor (1 year and 7 months on treatment) or the prior aromatase inhibitor (1 year and 9 months on treatment). We did not have a pre-CDK4/6i biopsy for the other two alterations of interest (*MTOR*^{T197R}, double *PIK3CA*^{E545K,G1007R}), so we could not verify if they were acquired/enriched.

To further test the potential of these mutations as drivers of resistance, we looked at whether these samples have other known alterations associated with CDK4/6i resistance. For the activating *BRAF*^{V600E} mutation (patient 23), the tumor had no other clonal acquired alterations, but did show loss of ER expression, making it difficult to tease out the degree of this mutation's resistance effect. For the activating *MTOR*^{T197R} mutation (patient 22), the biopsy also had an *FGFR1* high amplification, which partly confounds the role of this mutation in resistance. Note that *FGFR1* amplification appears to not always drive resistance to CDK4/6i on its own, since it often co-occurs with other resistance-associated alterations⁵. For the double *PIK3CA*^{E545K,G1007R} mutation (patient 19), the biopsy had an activating *ESR1* mutation, a known resistance mechanism to endocrine therapy, but did not have any known alterations associated with CDK4/6i resistance. None of these biopsies had additional known oncogenic mutations in the PI3K/AKT/mTOR, MAPK, or RTK pathways (patient 22 had an *FGFR1* high amplification, but no known oncogenic mutations), known oncogenic mutations or high-grade copy number alterations (CNA) in cell cycle genes associated with CDK4/6i resistance (*RBI*, *CCNE1*, or *CDK6*), or loss-of-function alterations in *FAT1*. Overall, the alterations co-occurring with the mutations we identified as potential resistance mechanisms are consistent with their proposed roles as drivers of CDK4/6i resistance, even if some of the co-occurring alterations confound their effect (Fig. 2).

Baseline ctDNA identified actionable genomic alterations not found in baseline tumor samples

For 11 patients, we obtained WES of both baseline tumor biopsies and baseline ctDNA. We leveraged this redundancy in our genomic data to verify the consistency between the tumor and ctDNA WES, and to see what additional information we could learn from having WES from both sources. Focusing on genes in pathways associated with resistance to endocrine therapy and CDK4/6i, we found few differences between the genomic alterations in 9 patients ($n = 9/11$, 82%) (Supplementary Fig. 1). Most of the differences we identified in these 9 patients were consistent with the higher sensitivity expected from tumor biopsies as compared to blood biopsies, particularly for CNAs. For example, the loss-of-function *RBI* mutations in patient 10 (subclonal) and 37 (clonal) were identified in the tumors but not in the ctDNA samples. In addition, we found evidence of biallelic inactivation (loss of heterozygosity and a loss-of-function mutation) for multiple tumor suppressors (*PTEN*, *TP53*, *NFI*) in the tumor but not in ctDNA samples, in which we could only identify the loss-of-function

mutations. There were a few cases where some alterations were identified in the ctDNA samples but not the tumors in these 9 patients, all of which involved subclonal mutations or CNAs, and which include a subclonal *TP53* loss-of-function mutation and *FGFR1* amplifications in 3 samples. We also looked for differences between the identified genomic alterations when looking at mutations with a known oncogenic effect in cancer genes and found no additional differences between the samples of these 9 patients.

For the other 2 patients ($n = 2/11$, 18%), patients 22 and 32, we identified mutually exclusive clonal driver mutations in cancer genes between the ctDNA and the tumor biopsy pair (Fig. 2C). Each sample pair shared truncal clonal mutations, indicative of a co-existence of multiple tumor lineages in the patient's cancer. For patient 22, we found a truncal *GATA3*^{M400fs} loss-of-function mutation with a clonal activating *MTOR*^{T197R} mutation in the ctDNA sample and a clonal activating double *ESR1*^{Y537S,L536P} mutation in the tumor sample. For patient 32, we found a truncal *PIK3CA*^{H1047L} mutation with a high-clonality activating *ERBB2*^{L755S} mutation in the ctDNA sample and a clonal activating *ERBB2*^{L869R} mutation in the tumor sample. The *MTOR*^{T197R} and *ERBB2*^{L755S} mutations found only in the blood biopsies are each clinically actionable and are associated with response to mTOR inhibitors like everolimus^{21–24} and the pan-HER kinase inhibitor neratinib, respectively^{25,26}. Based on this and additional evidence, OncoKB classifies *MTOR*^{T197R} as a mutation with compelling biological evidence (OncoKB Level 4) and *ERBB2*^{L755S} as a mutation with compelling clinical evidence (OncoKB Level 3a). Thus, we identified clinically actionable clonal mutations in the ctDNA but not in the tumor baseline biopsy of 2 patients that are each likely to be the mechanism of resistance.

Consistent transcriptomic features in genes associated with resistance to CDK4/6 inhibitors and endocrine therapy

The genomic landscape of baseline tumor biopsies in this trial spanned the spectrum of genes and pathways (RTK, MAPK, PI3K/AKT/mTOR, cell cycle, and ER pathways) known to be associated with resistance to CDK4/6 inhibitors and endocrine therapy (Fig. 2). Motivated by this finding, we hypothesized that genomic alterations in these resistance genes and pathways (in particular, known oncogenic mutations and high-grade CNAs) would have a corresponding high level of transcriptional signature activity (for oncogenic mutations and possibly for high-grade CNAs) or gene expression (for genes with high-grade CNAs). We also hypothesized that some of these genomic alterations and transcriptional signatures could correlate with the intrinsic molecular subtype (PAM50) of tumor samples. To test these hypotheses, we leveraged the genomic and transcriptomic data of the baseline tumor biopsies (14 biopsies with both WES and RNA-seq). Because of the modest size of our cohort, we focused on the genes we and others had previously identified to be associated with resistance (those in Fig. 2), transcriptional signatures from the 50 Hallmark gene sets, and 3 RTK transcriptional signatures from our recent work on resistance to endocrine therapy^{11,12}. These 3 RTK signatures are associated with transcriptional activity of HER2 mutants (HER2 MUT), FGFR (FGFR ACT), or a combination of both signatures (RTK ACT).

In order to quantify whether the expression of a gene or the activity of a transcriptional signature has a high or low value, we needed a cohort to serve as a reference for gene expression. Given that these tumor samples come from patients with HR + /HER2- MBC, we also needed a reference gene expression cohort that is receptor status-balanced in order to accurately assign a molecular subtype (research-grade PAM50)²⁷. For these purposes, we used the Metastatic Breast Cancer Project (MBCProject), which has genomic (WES, $n = 379$ tumor samples), transcriptomic (RNA-seq, $n = 200$ tumor samples) and clinical data (including receptor status: 84 HR + /HER2-, 27 HR + /HER2+, 10 HR-/HER2+, 12 HR-/HER2-), as the reference cohort²⁸. After assigning a molecular subtype to the 14 biopsies in this trial, we found that

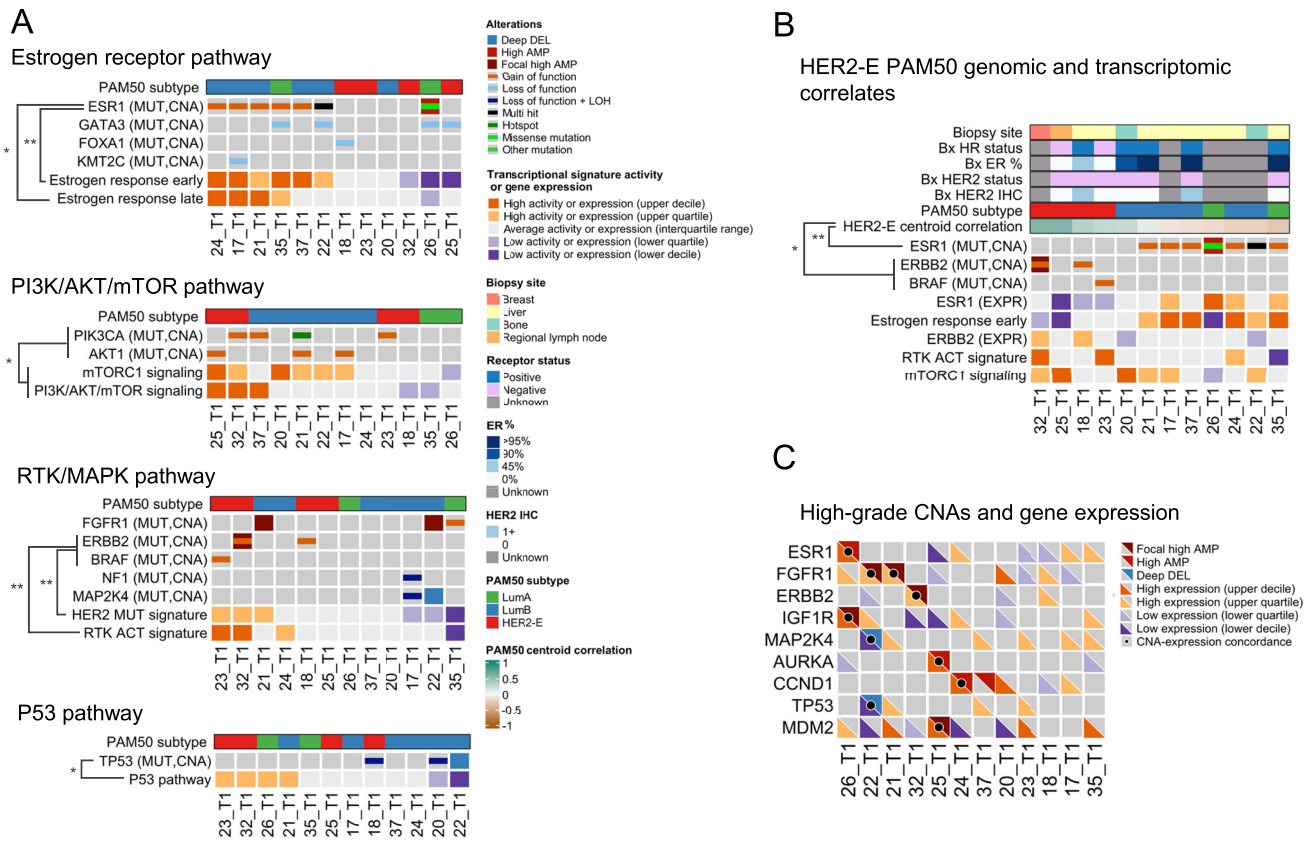


Fig. 3 | Consistency between genomic and transcriptomic features in genes associated with CDK4/6 inhibitors and antiestrogen treatment resistance. Joint genomic and transcriptomic analysis was performed on all baseline trial tumor biopsies with both WES and RNA-seq and a non-Normal PAM50 subtype ($n = 12$ samples and patients). **A** A comutation plot (CoMut) shows the consistency between the presence of oncogenic alterations and the activity of transcriptional signatures of their associated signaling pathway. Distinct genes and signatures are displayed, depending on the pathway (ER, PI3K/AKT/mTOR, RTK/MAPK, and P53). For each pathway, only genes from Fig. 2 with at least one known oncogenic mutation in the samples with transcriptomic data are shown. Biopsies are ordered based on the combined activity of the pathway signatures. **B** A CoMut displays the association between the presence of oncogenic mutations in *ERBB2* or *BRAF* and a HER2-enriched subtype, and oncogenic mutations in *ESR1* and a Luminal A or B subtype. Biopsies are ordered based on their correlation to the HER2-enriched centroid. Additional features shown are clinical and RNA-seq-based measures of ER and HER2 activity (HR and HER2 receptor status, ER percentage by IHC, HER2 IHC score, *ESR1* and *ERBB2* gene expression, and activity of the RTK ACT and estrogen response early transcriptional signatures) and biopsy site. An expanded version of (A) and (B) with additional clinical, genomic, and transcriptomic features is included in Supplementary Fig. 2. **C** A CoMut shows the concordance between high-

grade CNA and gene expression levels. Cases with CNA and gene expression concordance (high amplification or focal high amplification and upper quartile or decile expression; deep deletion and lower quartile or decile expression) are indicated with a black dot. Quantiles for transcriptional signature activity and gene expression levels are derived from MBCProject. Statistically significant associations between signature activities and known oncogenic mutations in (B) and (C) are denoted with asterisks (one-sided Mann–Whitney test). *ESR1* activating mutations vs estrogen response early ($AUC = 1.00$, $P = 1.08 \times 10^{-3}$), *ESR1* activating mutations vs estrogen response late ($AUC = 0.86$, $P = 2.06 \times 10^{-2}$, one-sided Mann–Whitney test), PI3K/AKT/mTOR activating pathway mutations vs combined activity of mTORC1 signaling and PI3K/AKT/mTOR signaling ($AUC = 0.83$, $P = 3.25 \times 10^{-2}$), grouped *ERBB2* or *BRAF* activating mutations vs RTK ACT signature ($AUC = 0.96$, $P = 9.09 \times 10^{-3}$), grouped *ERBB2* or *BRAF* activating mutations vs HER2 MUT signature ($AUC = 0.96$, $P = 9.09 \times 10^{-3}$), grouped *TP53* biallelic inactivation and deep deletions vs P53 pathway signature ($AUC = 0.93$, $P = 1.81 \times 10^{-2}$), grouped *ERBB2* and *BRAF* activating mutations vs HER2-E PAM50 centroid ($AUC = 0.93$, $P = 1.82 \times 10^{-2}$), and activating *ESR1* mutations vs HER2-E PAM50 centroid ($AUC = 0.92$, $P = 7.58 \times 10^{-3}$). (*) $P < 0.05$, (**) $P < 0.01$. Source data are provided as a Source Data file.

2 samples had a Normal PAM50 subtype, which is indicative of a low tumor content, so we excluded these samples from the joint genomic and transcriptomic analysis (resulting in $n = 12$ biopsies with both WES and RNA-seq and a non-Normal PAM50 subtype).

In agreement with our hypothesis, joint genomic and transcriptomic analysis revealed a high degree of consistency between the presence of known oncogenic mutations and the activity of transcriptional signatures of these pathways (Fig. 3A, Supplementary Fig. 2A). In particular, activity of each of these transcriptomic signatures was a strong classifier for the presence of oncogenic mutations in the respective pathways, as described in more detail below. Oncogenic mutations were also enriched in tumors with high activity in the transcriptomic signatures. These effects were particularly strong for *ESR1* activating mutations in the ER pathway and to a lesser degree with

activating mutations in the PI3K/AKT/mTOR pathway (*AKT1* or *PIK3CA*) or the RTK/MAPK pathways (*ERBB2* or *BRAF*) (Fig. 3).

For the ER pathway, activity in the ER pathway Hallmark signatures were a strong classifier for the presence of *ESR1* activating mutations (estrogen response early, $AUC = 1.00$, $P = 1.08 \times 10^{-3}$; estrogen response late $AUC = 0.86$, $P = 2.06 \times 10^{-2}$, one-sided Mann–Whitney test) (Fig. 3A, top). *ESR1* activating mutations ($n = 6/12$, 50% of biopsies) were enriched in tumors with high activity in the estrogen response early signature ($n = 6/12$, 50%; $P = 2.16 \times 10^{-3}$, two-sided Fisher exact test). This effect was similar but not statistically significant for the estrogen response late signature ($n = 6/12$, 50%; $P = 6.06 \times 10^{-2}$, two-sided Fisher exact test).

For the PI3K/AKT/mTOR pathway, combined activity of mTORC1 signaling and PI3K/AKT/mTOR signaling signatures was

statistically significant as a classifier for the presence of grouped activating PI3K/AKT/mTOR pathway mutations (only *AKT1* and *PIK3CA* mutations for these samples) ($AUC = 0.83$, $P = 3.25 \times 10^{-2}$, one-sided Mann–Whitney test) (Fig. 3A, middle top). None of these comparisons were statistically significant when looking at each of these signatures or activating mutations individually, or when looking at tumors with high activity in these signatures (all comparisons $P > 5.00 \times 10^{-2}$), although activity in the mTORC1 signaling signature was borderline statistically significant as a classifier for activating *AKT1* mutations ($AUC = 0.85$, $P = 5.00 \times 10^{-2}$, one-sided Mann–Whitney test).

For the RTK/MAPK pathway, activity of the RTK ACT or HER2 MUT signatures was each a good classifier for the presence of grouped activating *ERBB2* or *BRAF* mutations ($AUC = 0.96$, $P = 9.09 \times 10^{-3}$, one-sided Mann–Whitney test for each signature) (Fig. 3A, middle bottom). None of these comparisons were statistically significant when taking each of these activating mutations individually and there was no statistically significant enrichment of these mutations when looking at tumors with high activity in RTK/MAPK signatures (all comparisons $P > 5.00 \times 10^{-2}$). Other known RTK/MAPK alterations (*NFI* biallelic inactivation, *FGFR1* activating mutations and high amplifications) were not associated with high activity in the RTK/MAPK signatures and seemed to inversely correlate with these signatures (Fig. 3A, Supplementary Fig. 2). As detailed below, the lack of association with RTK/MAPK signatures in these individual cases could be related to the presence of concurrent activating *ESR1* mutations in those tumors (17_T1, 21_T1, 22_T1, 35_T1).

As an additional consistency check, we verified that deactivating *TP53* alterations (biallelic inactivation, $n = 2/12$, 17%; deep deletions, $n = 1/12$, 8%) were associated with P53 pathway activity (Fig. 3A bottom). Activity in the P53 pathway signature was a statistically significant classifier for the presence of grouped *TP53* biallelic inactivation and deep deletions ($AUC = 0.93$, $P = 1.81 \times 10^{-2}$, one-sided Mann–Whitney test). Similarly, these *TP53* alterations were enriched in samples with low P53 pathway signature activity ($P = 4.54 \times 10^{-2}$, two-sided Fisher's exact test).

Given the observed association of activating *ERBB2* and *BRAF* mutations with RTK/MAPK pathway transcriptional signature, we hypothesized this association could be related to the PAM50 subtype of these tumor samples. Consistent with this hypothesis, grouped *ERBB2* and *BRAF* mutations were exclusive to tumors with a HER2-Enriched (HER2-E) PAM50 subtype ($n = 4/12$, 33%), in which they were enriched ($P = 1.82 \times 10^{-2}$, two-sided Fisher exact test), and correlation to the HER2-E PAM50 centroid was a good classifier for the presence of these mutations ($AUC = 0.93$, $P = 1.82 \times 10^{-2}$, one-sided Mann–Whitney test) (Fig. 3B). In addition, correlation to the HER2-E PAM50 centroid was a good classifier for the absence of activating *ESR1* mutations ($AUC = 0.92$, $P = 7.58 \times 10^{-3}$, one-sided Mann–Whitney test). Unlike the HER2-E PAM50 centroid, the RTK ACT or HER2 MUT signatures were not statistically significant classifiers for activating *ESR1* mutations ($P > 5.00 \times 10^{-2}$). Activating *ESR1* mutations were exclusive to samples with a Luminal A ($n = 2/12$, 17%) or B ($n = 6/12$, 50%) subtype and were absent in the tumors with *ERBB2* and *BRAF* mutations. Mutual exclusivity between activating mutations in *ESR1* and *ERBB2* or *BRAF* is consistent with prior work in HR+/HER2- MBC^{5,11,12,16}. Only very recently has a similar association been reported between activating mutations in the RTK/MAPK pathway or *ESR1* and the PAM50 molecular subtype of a tumor in HR+/HER2- MBC²⁹.

To verify the consistency between high-grade CNAs (high amplifications, deep deletions) and gene expression, we looked at whether tumors with high-grade CNAs had a corresponding high or low level of gene expression. For 9 out of 10 high-grade CNAs there was a corresponding high or low level of expression in these genes (Fig. 3C), which included *FGFR1* ($n = 2/12$, 17%), *ESR1* ($n = 1/12$, 8%), *ERBB2* ($n = 1/12$, 8%), *IGFIR* ($n = 1/12$, 8%), and *AURKA* ($n = 1/12$, 8%), among others.

Conversely, for the majority of cases with an above-average level of expression in these genes, there were no corresponding high-grade CNAs (52 total gene/tumor cases, 9 of which had a high-grade CNA), a result that is consistent with recent work³⁰. These results support the often-used assumption that high-grade CNAs in resistance-associated genes have a strong effect on their expression but highlight how above-average expression levels do not often have an associated high-grade CNA.

In summary, we found that multiple genomic resistance mechanisms in the ER, RTK/MAPK, and PI3K/AKT/mTOR pathways, such as activating mutations in *ESR1*, *ERBB2*, or *AKT1* and *FGFR1* amplifications, have specific transcriptomic features (pathway transcriptional signatures, gene expression levels) associated with them. Specifically, there was a statistically significant association between *ESR1* mutations and ER pathway Hallmark signatures, *ERBB2*/*BRAF* mutations and the RTK ACT or HER2 MUT signatures, and the presence of *ERBB2*/*BRAF* or absence of *ESR1* mutations and the HER2-E centroid correlation. These results suggest that these transcriptomic features could be used to identify the pathways driving CDK4/6i and endocrine resistance in a tumor.

Combined genomic and transcriptomic features in baseline biopsies identify likely mechanism of resistance to prior CDK4/6 inhibitor and endocrine therapy treatments in nearly every patient

The genomic and transcriptomic analysis of baseline biopsies identified known and potential features associated with the resistance to CDK4/6 inhibitors and endocrine therapy. These features include activating mutations in *ESR1*, *ERBB2*, *FGFR1*, *AKT1*, *BRAF*, and *MTOR*; double *PIK3CA* activating mutations; loss-of-functions mutations in *NFI*, *RBI*, and *PTEN*; amplifications in *FGFR1*, *FGFR2*, *ERBB2*, and *AURKA*; ER loss; and transcriptional features such as the HER2-E subtype, high transcriptional activity of ER signatures, or high RTK activity (high expression of RTKs or high RTK signature activity).

Based on these and additional features, we asked whether these known and plausible resistance mechanisms could explain each baseline tumor's resistance to prior CDK4/6i and antiestrogen treatments. Additional features we considered include known resistance features such as the Basal PAM50 subtype¹⁰ and plausible resistance features, some of which have preliminary studies that associate them to reduced sensitivity to CDK4/6i and endocrine therapy, such as amplification or high expression of *IGFIR* or *INSR*^{12,31,32}, and low ER activity (low *ESR1* expression or low ER pathway signature activity)³.

For 22 out of 23 patients with WES and/or RNA-seq of a baseline biopsy ($n = 22/23$, 96%), we identified genomic or transcriptomic features that could explain the tumor's resistance to CDK4/6i or anti-ER treatments (Fig. 4, Supplementary Fig. 3, Supplementary Data 6). Fourteen patients ($n = 14/23$, 61%) had known resistance mechanisms to both of these treatments (i.e., published evidence of a mechanistic role in resistance to these treatments), 3 patients ($n = 3/23$, 13%) had a combination of known and plausible mechanisms, and 5 patients ($n = 5/23$, 22%) had only plausible mechanisms (i.e., preclinical or theoretical evidence suggesting a role in resistance). Given that the resistance mechanisms identified for each patient can be based on clinical, genomic, or transcriptomic features, we looked at how often each mechanism explained the tumor's treatment resistance. In particular, we focused on the cases where oncogenic mutations in resistance genes, clinical features, or transcriptomic features alone could explain treatment resistance (Fig. 4).

The chart encodes whether key features associated with resistance to CDK4/6 inhibitors or anti-estrogen treatment are seen in the trial baseline biopsies of patients with either WES or RNA-seq of a baseline sample ($n = 23$ patients). For each patient, it includes whether these features could explain if the baseline tumor is resistant to prior

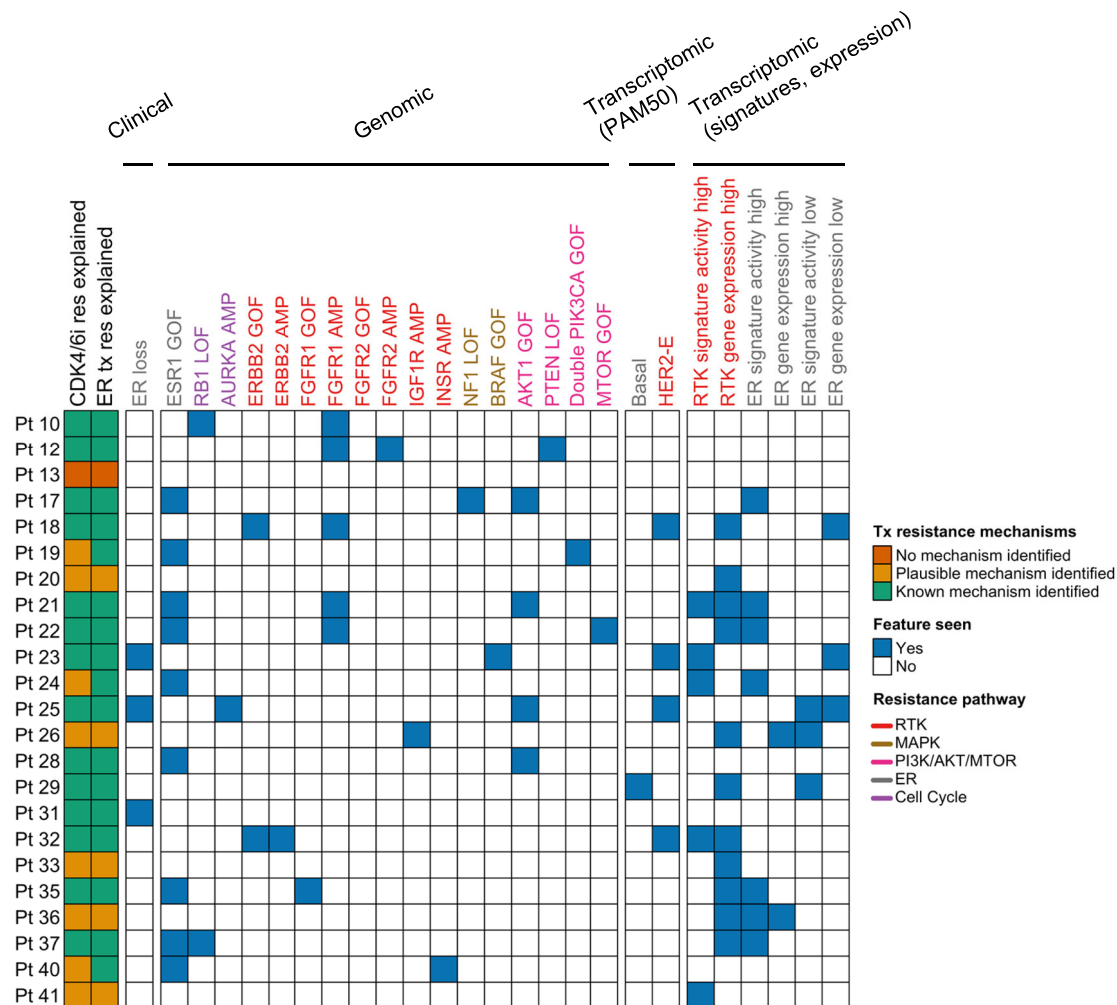


Fig. 4 | Clinical, genomic, and transcriptomic features can explain resistance to CDK4/6 inhibitors and antiestrogen treatment in patient's tumors. $n = 23$ patients. GOF gain of function mutation, LOF loss of function mutation, AMP high amplification, Pt patient. Source data are provided as a Source Data file.

CDK4/6i and antiestrogen treatments, and if these are known or plausible resistance mechanisms. For 22 out of 23 patients a known or plausible resistance mechanism was identified. Features included are based on clinical assays (loss of ER measured by IHC), genomic data (known oncogenic mutations and high-grade amplifications in known or plausible resistance genes), and transcriptomic data (Basal subtype, HER2- enriched subtype, high expression or activity in an RTK gene or RTK signature, high/low expression or activity in *ESR1* or an ER pathway signature). Features are colored based on the resistance signaling pathway they are associated with. A modified version of this figure that groups these features by gene and signaling pathway, and includes the data types available for each patient is included in Supplementary Fig. 3. The transcriptional signature activity of the Hallmark gene sets and RTK transcriptional signatures for these tumors is shown in Supplementary Fig. 4.

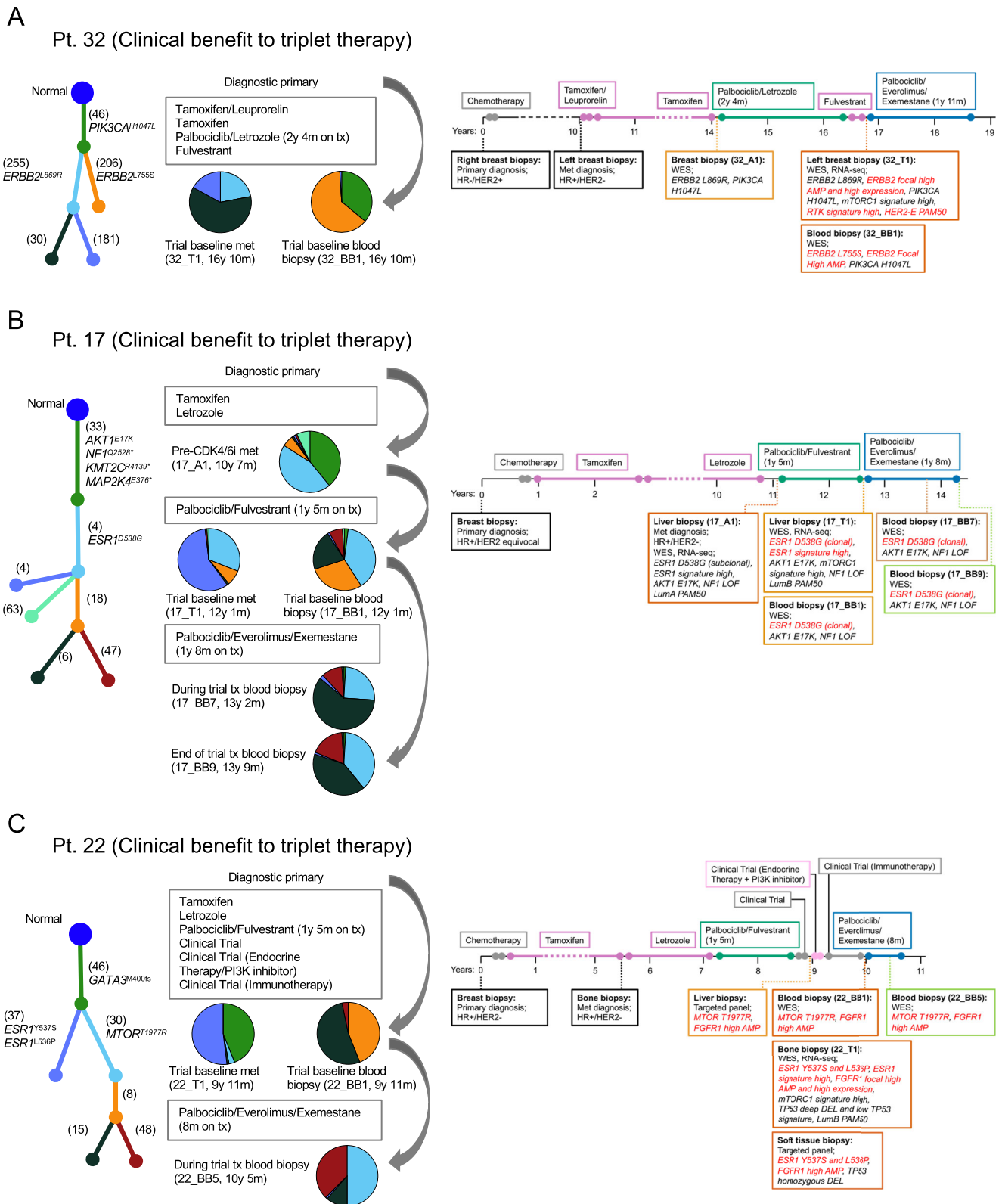
For 13 patients ($n = 13/23$, 57%), resistance to both treatments could be explained solely by considering oncogenic mutations in known (*ESR1*, *AKT1*, *PTEN*, *NF1*, *FGFR1*, *ERBB2*, *RBI*) or plausible resistance genes (*BRAF*, *MTOR*, double mutations in *PIK3CA*), or ER loss (pts. 23, 25, and 31). For 5 patients ($n = 5/23$, 22%; 4 with no genomic data), the resistance mechanisms identified were solely transcriptomic features: Basal PAM50 subtype (along with high RTK signature activity and low ER activity) in patient 29, high RTK activity (*IGF1R* expression) and ER activity (high estrogen response early signature activity) in patient 36, and high RTK activity in patients 20 (high *FGFR1* expression), 33 (high *IGF1R* expression), and 41 (high activity of the RTK ACT

and HER2 MUT signatures). For 4 patients ($n = 4/23$, 17%), the resistance mechanisms identified included a combination of oncogenic mutations, high-grade CNAs, and transcriptomic features. For example, *FGFR1* amplification and *RBI* loss-of-function for patient10; an activating *ESR1* mutation and high activity of the RTK ACT signature for patient 24; and *IGF1R* amplification and high *IGF1R* expression, a *GATA3* loss-of-function mutation, and low ER activity (low signature activity of the estrogen response early and late signatures) for patient 26.

In summary, we found that in 22 out of 23 patients, we could identify known or plausible resistance mechanisms to the prior CDK4/6i and antiestrogen treatments by using the clinical, genomic, and transcriptomic features in their baseline tumors. This includes 5 patients in which the only mechanism identified was a transcriptomic feature, illustrating how transcriptomic data can provide complementary information not present in genomic data and provide insights even for cases when no genomic data is available.

Evolutionary analysis revealed convergent and divergent paths to CDK4/6i + anti-ER treatment resistance in tumors with distinct lineages

For 6 patients for whom we had WES from paired pre-treatment and post-resistance tumor samples (5 patients) or concurrent post-treatment tumor and ctDNA samples from distinct tumor lineages (2 patients), we wanted to identify the genomic alterations that were acquired or became enriched following the prior CDK4/6i treatment and that could be driving treatment resistance. To do this, we carried



out evolutionary analysis (tumor phylogeny, clonal dynamics) to identify acquired or enriched genomic alterations in the trial baseline sample(s) (which are post-CDK4/6i) as compared to the older, pre-CDK4/6i sample (Figs. 5 and 6). Note that we refer to high-clonality genomic alterations present in the post-CDK4/6i but not detected in the pre-CDK4/6i sample as acquired alterations, even though they might exist in the pre-CDK4/6i sample or prior tumors with very low clonality. To help contextualize the treatments these samples have

been exposed to (and, putatively, become resistant to), we also included a clinical case history for these patients (treatment sequence and duration, timing of biopsies and diagnoses) (Supplementary Data 7).

For all patients with a pre-CDK4/6i sample, we identified acquired or enriched genomic alterations in known resistance genes. For patient 32, the post-resistance tumor sample had a clonal *ERBB2*^{L869R} activating mutation that was also present in the pre-treatment sample, as well as

Fig. 5 | Tumor evolutionary analysis and clinical vignettes for patients who derived clinical benefit from palbociclib, everolimus, and exemestane triplet therapy. Analysis of tumor phylogeny and clonal dynamics following CDK4/6i and anti-ER therapy revealed convergent (HER2 activation) and divergent (ER or PI3K/AKT/mTOR activation) paths to treatment resistance in tumors with distinct lineages (A, B). Evolutionary analysis, acquired genomic alterations to prior CDK4/6i, and treatment history is shown for patients with pre-CDK4/6i and post-CDK4/6i (trial baseline) biopsies. **A** shows convergent evolution of *ERBB2* activation in two distinct co-existing tumor lineages (an activating clonal *ERBB2*^{L869R} mutation and an acquired *ERBB2* focal high amplification in 22_T1; an acquired activating high-clonality *ERBB2*^{L755S} mutation in 32_BB1). **B** shows an increase in the clonality of an activating *ESR1*^{D538G} mutation (from subclonal to clonal). **C** shows a case with two distinct co-existing tumor lineages in its post-CDK4/6i biopsies, each with clonal drivers mutations in divergent pathways (ER pathway with an activating clonal

ESR1^{Y537S,L536P} mutation in 22_T1; PI3K/AKT/mTOR pathway with an activating clonal *MTOR*^{T1977R} mutation in 22_BB1). Even though no pre-CDK4/6i biopsy was available for this patient, targeted panel data from other post-CDK4/6i biopsies confirmed the existence of these tumor lineages. In a patient's tumor phylogenetic tree, each subclone is associated with a branch and a color, and this color matches the color in the pie chart that quantifies the relative abundance of each subclone in the tumor. The number of mutations unique to each subclone and known oncogenic mutations are shown next to each branch. Data shown in the clinical vignettes includes the timing of treatments and biopsies, and selected clinical, genomic, and transcriptomic features. Time on treatment for CDK4/6i-containing therapies is included in the figure. Acquired genomic alterations (in A, B) or putatively acquired genomic alterations (in C) following CDK4/6i therapy are shown in red, together with their associated transcriptomic features.

an acquired *ERBB2* focal high amplification (copy number above ploidy from 1.9 to 9.7) not found in the pre-treatment sample. We did not detect *ERBB2*^{L869R} in the concurrent post-resistance ctDNA sample, and instead identified an acquired high-clonality *ERBB2*^{L755S} activating mutation that was not found in the pre-treatment sample (Fig. 5A). For patient 17, the post-resistance sample showed an enrichment in an activating *ESR1*^{D538G} mutation, which was subclonal in the pre-CDK4/6i samples but clonal in the post-CDK4/6i sample (Fig. 5B). For patient 23, the post-resistance sample had shared truncal mutations (*PIK3CA*^{E545K}, *CDH1*^{A824fs}, and others) and an acquired clonal *BRAF*^{V600E} activating mutation (Fig. 6A). For patient 21, the post-resistance sample had shared truncal alterations (mutations of unknown significance and a *FGFR1* focal high amplification) and an acquired clonal *ESR1*^{D538G} and *AKT1*^{E17K} activating mutations (Fig. 6B). For patient 26, the post-resistance sample had shared truncal alterations (SNVs of unknown significance and an *IGF1R* focal high amplification), an acquired subclonal *GATA3*^{412fs} truncating mutation, an acquired clonal *ESR1*^{H524L} missense mutation, and an increased amplification in *ESR1* (copy number above ploidy from 5.9 to 7.6) that included the region with *ESR1*^{H524L} (Fig. 6C).

Of these patients, two had acquired or enriched genomic alterations only in the ER pathway (*ESR1*^{D538G} in Pt 17, Fig. 5B; *GATA3*^{412fs}, *ESR1*^{H524L}, and *ESR1* high amplification in patient 26, Fig. 5C) and no known acquired alterations associated with CDK4/6i resistance, which suggests that the mechanisms of resistance is primarily related to the endocrine partner.

For patients 22 and 32, in their baseline blood and tumor biopsies, we had identified mutually exclusive clonal driver mutations (Fig. 2C), evolutionary analysis confirmed the co-existence of multiple tumor lineages in each of these cancers (Fig. 5A, C).

For patient 32, the identified tumor lineages showed convergent evolution of *ERBB2* activation through distinct known activating mutations and the focal high amplification of *ERBB2* (Fig. 5A). The baseline tumor sample is dominated by a lineage with *ERBB2*^{L869R} and the baseline blood sample by a lineage with *ERBB2*^{L755S}, both sharing a truncal *PIK3CA*^{H1047L} mutation. The pre-CDK4/6i sample had clonal *ERBB2*^{L869R} and *PIK3CA*^{H1047L} mutations, and thus, shared the same lineage as the baseline tumor sample. Unlike the baseline samples, the pre-CDK4/6i tumor did not show an amplification of *ERBB2*, consistent with the original HR + /HER2- MBC diagnosis. The activation of *ERBB2* in the baseline tumor is also reflected in its transcriptional features: a HER2-E PAM50 subtype and high activity in the RTK ACT and HER2 MUT signatures. To our knowledge, convergent evolution of *ERBB2* activation following CDK4/6i and endocrine therapy treatment has not been previously reported. (Figs. 5, 6)

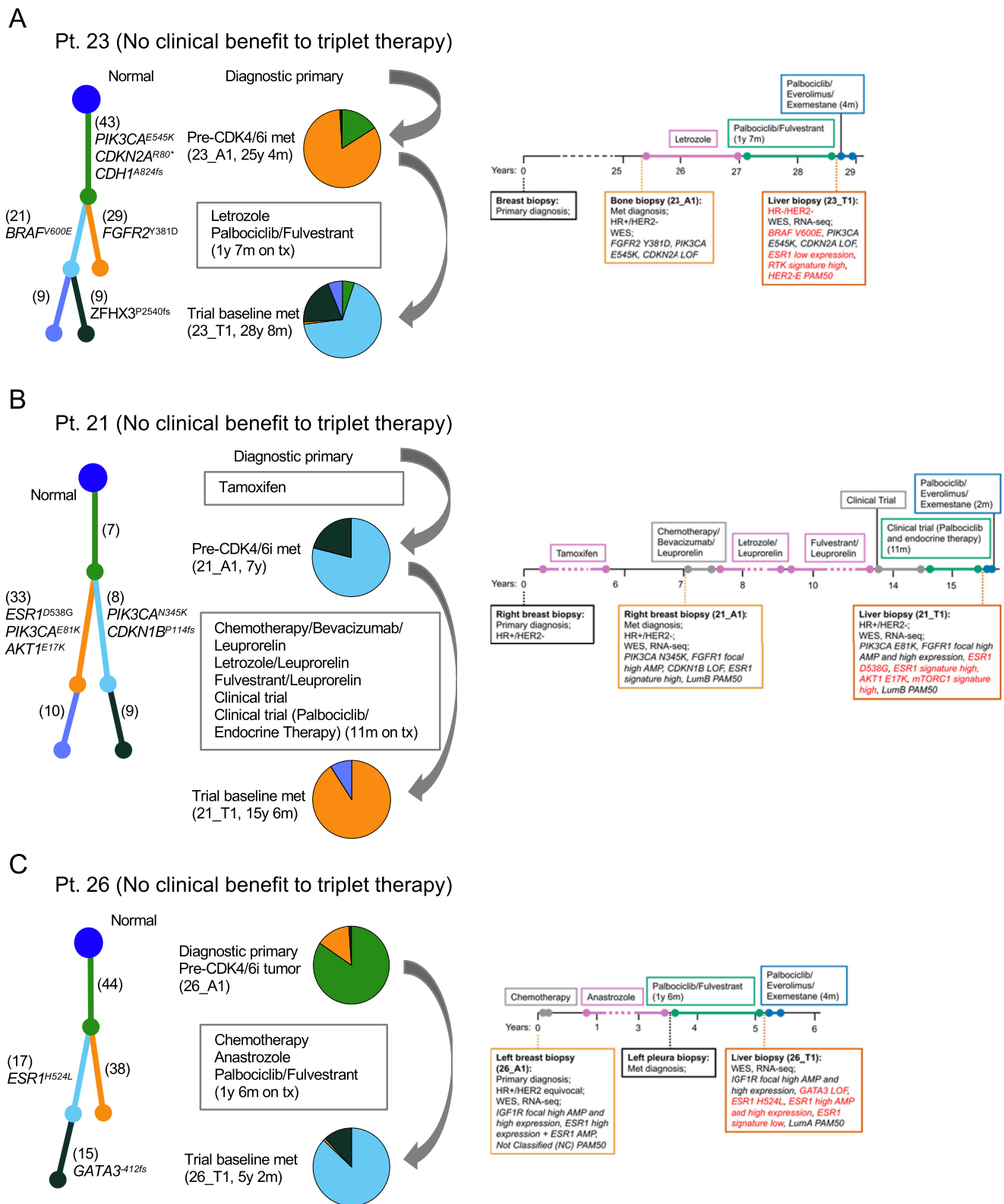
For patient 22, we identified two tumor lineages with clonal drivers mutations in divergent pathways: a double *ESR1*^{Y537S,L536P} mutation (ER pathway) in the tumor sample and an *MTOR*^{T1977R} mutation (PI3K/AKT/mTOR pathway) in the ctDNA sample (Fig. 5C). Both samples had a shared truncal *GATA3*^{M400fs} mutation and a shared *FGFR1* high

amplification, which was additionally classified as a focal high amplification for the tumor sample. Each of the baseline samples had known or plausible resistance mechanisms to CDK4/6 inhibitors and endocrine therapy (*ESR1*^{Y537S,L536P} and *FGFR1* amplification for 22_T1; *MTOR*^{T1977R} and *FGFR1* amplification for 22_BB1). Although we could not obtain a pre-CDK4/6i sample for this patient, we did verify that both lineages were observed in metastatic biopsies taken after CDK4/6i treatment and before beginning the trial regimen. These biopsies were profiled using targeted DNA sequencing (OncoPanel) and were from distinct metastatic sites than the baseline biopsy (liver and soft tissue vs. bone for the baseline biopsy). The soft tissue biopsy had a double *ESR1*^{Y537S,L536P} mutation, an *FGFR1* high amplification, and a *TP53* homozygous deletion, consistent with what we identified in the baseline tumor biopsy. The liver biopsy had an *MTOR*^{T1977R} mutation and an *FGFR1* high amplification, consistent with the ctDNA sample.

Overall, tumor evolutionary analysis identified acquired genomic alterations that we attributed to acquired CDK4/6i and endocrine therapy resistance. These acquired genomic alterations were in the RTK (*ERBB2* amplification, *ERBB2*^{L755S}), MAPK (*BRAF*^{V600E}), PI3K/AKT/mTOR (*AKT1*^{E17K}), or ER (*ESR1*^{H524L}, *ESR1*^{D538G}, *GATA3*^{412fs}) pathways. Finally, we identified co-existing tumor lineages with distinct driver mutations in resistance genes in two patients. In one of these patients, there was strong evidence for the convergent evolution of *ERBB2* activation following CDK4/6i therapy.

Response to combined palbociclib, everolimus, and exemestane was correlated with activation of the mTOR pathway

We looked for genomic and transcriptomic features in the baseline biopsies ($n = 23$ patients with either WES or RNA-seq of a baseline biopsy) that correlated with subsequent clinical benefit to the clinical trial of combined palbociclib + everolimus + exemestane ($n = 4/23$, 17%). Although there were no definite genomic correlates associated with the group that derived clinical benefit, (which was not surprising given the limited sample size), we did identify alterations in the PI3K/AKT/mTOR pathway as a plausible correlate. There were no clear group differences at the gene level, and many of the known mutations in resistance genes were found in both groups, including activating mutations in *ESR1*, *AKT1*, and *ERBB2*, and amplifications in *FGFR1* and *ERBB2* (Fig. 2). When looking at genomic alterations in pathways, we found that the tumors in the clinical benefit group all had a known oncogenic mutation in the PI3K/AKT/mTOR pathway (Fig. 7A). For patient 22, the ctDNA sample (22_BB1) had a clonal activating *MTOR*^{T1977R} mutation, which is consistent with the evidence linking this mutation with response to mTOR inhibitors such as everolimus^{21–24} (Figs. 2B, 5C). For patient 19, the ctDNA sample had a clonal activating double *PIK3CA*^{E545K,G1007R} mutation (19_BB1, Fig. 2D). Patients 17 and 32 had clonal activating *AKT1*^{E17K} and *PIK3CA*^{H1047L} mutations, respectively (17_T1 and 32_T1, Fig. 2B). Given that everolimus targets the PI3K/AKT/mTOR pathway, this suggests the observed association between response and PI3K/AKT/mTOR



mutations could be attributed to the everolimus component of combination therapy.

Given the observed association between PI3K/AKT/mTOR mutations and clinical benefit, we looked at possible reasons why this association was not observed for all the activating *AKT1^{E17K}* mutations. Two of the four patients with an *AKT1^{E17K}* mutant tumor had stable disease but discontinued the trial due to toxicity (Fig. 7A); of the remaining two patients, one derived clinical benefit (patient 17, stable

disease >24 weeks) while the other patient did not (patient 21, best response was progressive disease). Their main noteworthy genomic/transcriptomic difference is in their HER2 MUT signature activity (high for patient 21 and low for patient 17; both were *ESR1*-mutant, RTK/MAPK mutant, and had a Luminal B subtype). Thus, we were only able to fully evaluate whether *AKT1^{E17K}*-mutant tumors responded to combined palbociclib, everolimus, and exemestane for two cases and found a clinical benefit for one of these cases.

Fig. 6 | Tumor evolutionary analysis and clinical vignettes for patients who did not derive clinical benefit from palbociclib, everolimus, and exemestane tri-plet therapy. Evolutionary analysis, acquired genomic alterations to prior CDK4/6i, and treatment history are shown for these patients. **A** shows acquired clonal activating *BRAF*^{V600E} mutation concurrent with ER loss. Transcriptomic features (low *ESR1* expression, HER2-enriched PAM50, high RTK signature activity) are concordant with these acquired events. **B** shows clonal activating *AKT*^{E17K} and *ESR1*^{D538G} mutations. **C** shows clonal *ESR1*^{H1524L} mutation (variant of unknown significance), an acquired subclonal *GATA3*^{-412fs} truncating mutation, and an increased *ESR1*

amplification (from amplification to high amplification). In a patient's tumor phylogenetic tree, each subclone is associated with a branch and a color, and this color matches that in the pie chart that quantifies the relative abundance of subclones. The number of mutations unique to each subclone and known oncogenic mutations are shown next to each branch. Data shown in the clinical vignettes includes the timing of treatments and biopsies, and selected clinical, genomic, and transcriptomic features. Time on treatment for CDK4/6i-containing therapies is included in the figure. Acquired genomic alterations following CDK4/6i therapy are shown in red, together with their associated transcriptomic features.

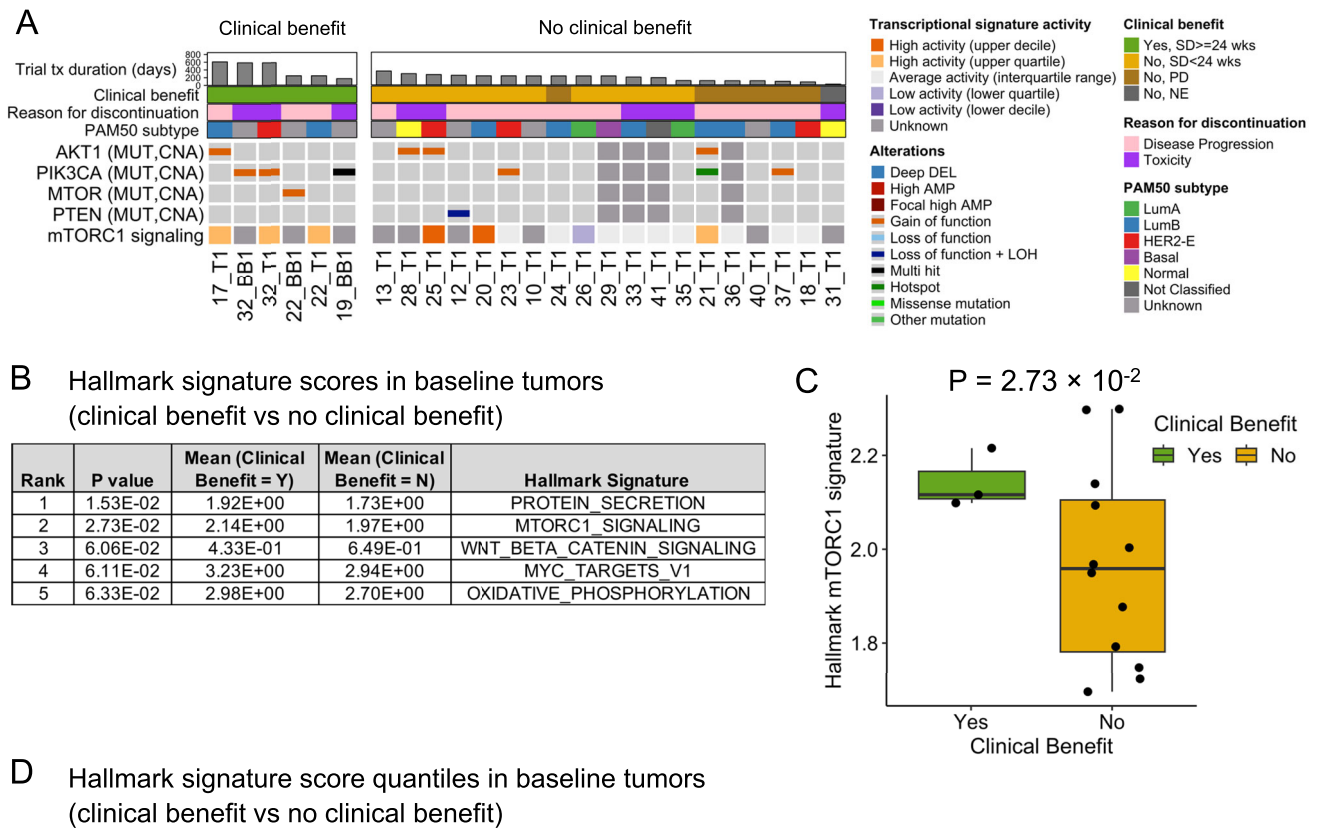


Fig. 7 | Correlation between mTOR pathway activity and response to triplet therapy in baseline tumor samples. **A** A co-mutation plot (CoMut) displays the putative association between clinical benefit to triplet therapy and the presence of genomic or transcriptomic features associated with PI3K/AKT/mTOR pathway activation. $n = 23$ patients. Each tumor and blood biopsy sample from patients that derived clinical benefit had either a known oncogenic mutation in *AKT1*, *PIK3CA*, or *MTOR*, or high activity of the mTORC1 signaling signature. Notably, two out of four patients with *AKT*^{E17K} mutations discontinued treatment because of toxicity. PI3K/AKT/mTOR pathway genes with at least one known oncogenic mutation are shown. Baseline tumor samples with either WES or RNA-seq are shown. Baseline blood biopsies were included when they were from a distinct lineage than the tumor biopsy (22_BB1, 32_BB2) or when there were no sequenced tumor biopsies (19_BB1). Biopsies are ordered by treatment duration on triplet therapy. (B-D) show top

results from comparing Hallmark signature activity in baseline tumor biopsies, with or without clinical benefit. The mTORC1 signaling signature is one of the top signatures associated with clinical benefit. **B**, **C** show Welch's *t*-test (two-sided) results and Hallmark signature activity for mTORC1 signaling, respectively (clinical benefit, $n = 3$ samples and patients; no clinical benefit, $n = 12$ samples and patients). **D** displays Fisher exact test (two-sided) results, comparing enrichment of tumors with a Hallmark signature activity in the upper or lower quartiles (clinical benefit, $n = 3$ samples and patients; no clinical benefit, $n = 12$ samples and patients). The Hallmark signatures contain 50 gene sets in total. Quantiles for transcriptional signature activity are derived from MBCProject. Boxplots span the interquartile range (IQR: 25–75th percentile) and have a center line denoting the median. Boxplot whiskers indicate the $1.5 \times IQR$ below or above the boxplot span. Source data are provided as a Source Data file.

Consistent with the association between PI3K/AKT/mTOR mutations and clinical benefit, transcriptomic analysis identified a correlation between mTORC1 pathway activity and clinical benefit. mTORC1 signaling signature activity was higher in samples with clinical benefit ($P = 2.73 \times 10^{-2}$, two-sided Welch's *t*-test) and

was top 2 among all Hallmark signatures (Fig. 7B, C, Supplementary Data 8). A similar result was found when looking at enrichment of high or low activity of Hallmark signatures and clinical benefit, that is, samples with high activity in mTORC1 signaling were enriched in those associated with clinical benefit

($P = 2.20 \times 10^{-2}$, two-sided Fisher exact test) (Fig. 7A, D, Supplementary Data 8).

In summary, we found early evidence that clinical benefit to palbociclib + everolimus + exemestane is correlated with activation of the mTOR pathway, namely, PI3K/AKT/mTOR mutations and mTORC1 pathway activity. (Fig. 7).

Discussion

In this study, we analyzed multi-omic and clinical data from patients diagnosed with metastatic HR+/HER2- breast cancer who had progressed on a prior CDK4/6 inhibitor, and were treated with a CDK4/6i-containing triplet therapy (palbociclib + everolimus + exemestane) as part of a phase Ib/2 clinical trial. This clinical trial evaluating the benefit of continued CDK4/6 therapy after progression on a prior CDK4/6 inhibitor is to our knowledge unique in having carried out in-depth multi-omic tumor analysis in baseline metastatic tissue and blood samples taken after development of CDK4/6i resistance. Although the CBR of 18.8% did not meet the pre-specified threshold (CBR \geq 65%), the multi-omic data from this trial provided a unique opportunity to study both the landscape of resistance to CDK4/6 inhibitors and correlates of response to subsequent therapy with combined palbociclib, everolimus, and exemestane. Unlike most prior studies on CDK4/6 inhibitor resistance, which focused exclusively on tumor DNA, our study explored both the DNA landscape (via WES) and the transcriptomic landscape (via RNA-seq), using both tumor biopsies and ctDNA.

We explored the differences in clinical benefit rate between triplet therapy clinical trials and potential factors behind them. Our clinical trial results stand in contrast to the phase I/II TRINITY-1 trial, in which the triplet of ribociclib + everolimus + exemestane resulted in a CBR of 65.2% or 59.4% by arm in their final efficacy analysis³³. Although both trials had relatively similar eligibility criteria, the patient population differed in important aspects. In particular, the patient population in our trial was more heavily pretreated both in terms of prior endocrine therapies (53% with 2 or more lines vs. 22% in TRINITY-1) and prior chemotherapy (38% vs. 13% in TRINITY-1)³⁴. Concordantly, we also found a larger proportion of *ESR1* mutations at baseline in our trial (47% of patients with a known activating mutation vs. 34% in TRINITY-1 with any *ESR1* mutation)³⁴. The CBR of our trial was also lower than the CBR of 40% from BOLERO-2¹⁹, although the patient population between them is different given that the latter were never exposed to CDK4/6 inhibitors. When compared to the EMERALD trial³⁵, whose standard-of-care group has a comparable exposure history as ours, we see a relatively similar CBR between them (18.8% vs. 24-week CBR 13.5% in EMERALD).

Another important difference between these trials is that the pattern of CDK4/6i re-exposure is different: in both trials a great majority of patients had previously received palbociclib (94% here vs. 100% in TRINITY-1) and very few had previously received either abemaciclib or ribociclib (6% here vs. 13% in TRINITY-1)³⁴. This means that in our trial most patients were re-exposed to the same CDK4/6i, while in TRINITY-1 they were predominantly exposed (i.e., switched) to a different one, a notable difference that could help explain the conflicting trial results.

Recent work on CDK4/6i re-exposure is consistent with the switch of CDK4/6i playing an important role in response to therapy. A multicenter retrospective analysis of abemaciclib exposure after progression on palbociclib found an unexpected benefit from abemaciclib, with a median PFS of 5.3 months and a treatment duration of \geq 6 months for 37% of patients³⁶. In MAINTAIN, a phase II randomized trial on CDK4/6i-resistant patients evaluating the switch of anti-estrogen therapy and either ribociclib or placebo, most patients also switched to a different CDK4/6i (11% of the full cohort had prior ribociclib), and they found a statistically significant improvement in the ribociclib arm compared to the placebo arm (median PFS of 5.33 vs. 2.76 months, respectively)³⁷. Although in vitro and in vivo work suggest

that ribociclib and palbociclib have similar pharmacological profiles and only abemaciclib differs from them (because of its CDK2 and CDK9 activity)^{38,39}, the results of MAINTAIN, and the large difference in CBR between our trial and TRINITY-1 (18.8% vs. 65.2% or 59.4%) points to the possibility that switching between distinct CDK4/6 inhibitors might be a strong contributor to this difference.

Our study found that oncogenic signaling pathways associated with CDK4/6i resistance were recapitulated by joint genomic and transcriptomic analysis. The DNA alterations found in the trial baseline biopsies (post-CDK4/6i, pre-triplet therapy; Fig. 2) captured the spectrum of genes and pathways comprising the known genomic landscape of CDK4/6i resistance. These alterations include oncogenic mutations known to be resistance mechanisms to CDK4/6 inhibitors and endocrine therapy: *AKT1* (PI3K/AKT/mTOR pathway), *NFI* (MAPK pathway), *ERBB2* (RTK pathway), *RBI* (cell cycle), and *ESR1* (ER pathway) (Fig. 2). Our analysis additionally identified plausible mechanisms of resistance in the MAPK pathway (an activating *BRAF*^{V600E} mutation) and in the PI3K/AKT/mTOR pathway (an activating *MTOR*^{T197R} mutation and an activating double *PIK3CA*^{E545K,G1007R} mutation, although we did not have a pre-CDK4/6i biopsy to verify these PI3K/AKT/mTOR mutations were acquired). An in-depth look at the alterations co-occurring with these potential resistance mechanisms showed some possible confounder alterations, but was overall supportive of their proposed role as CDK4/6i-resistance drivers.

Through joint analysis of genomic and transcriptomic tumor data, we discovered a high degree of consistency between the presence of known genomic resistance mechanisms (mutations, high-grade CNAs) and their associated transcriptomic features (gene expression levels, transcriptional signature activities, molecular subtype) (Fig. 3). In particular, we found that all biopsies with activating mutations in *ESR1* showed a concordant high activity in ER pathway signatures, and we also saw an analogous but less strong effect for activating mutations in the PI3K/AKT/mTOR pathway (*AKT1* or *PIK3CA*) and the RTK/MAPK pathway (*ERBB2* or *BRAF*) (Fig. 3A).

The consistency between genomic resistance mechanisms and their associated transcriptomic features suggested some of these features could be used to identify the genes or pathways driving CDK4/6i and endocrine therapy resistance in tumors, particularly in those without genomic data or clear genomic drivers. Using the clinical, genomic, and transcriptomic features in their baseline tumors, we identified known or plausible resistance mechanisms to the prior CDK4/6i and anti-ER therapies for 22 out of 23 patients. This included 5 patients in which the only mechanism identified was a transcriptomic feature: 4 patients with no genomic data, and 1 patient with genomic data but no clear genomic drivers. These results highlight how genomic and transcriptomic data complement each other and can identify putative drug resistance drivers in tumors.

Our study found a potential association between genomic alterations driving resistance and transcriptomic-based molecular subtype. A notable finding from our genomic/transcriptomic analysis was that activating *ESR1* mutations were exclusive to samples with a Luminal A or B subtype and that activating *ERBB2* or *BRAF* mutations were exclusive to samples with a HER2-E subtype, making these groups mutually exclusive (Fig. 3B). This mutual exclusivity between *ESR1* and RTK/MAPK pathway mutations is consistent with previous observations in HR+/HER2- MBC^{11,12,16}. To our knowledge, the presence of these oncogenic mutations had not been linked to the PAM50 molecular subtype of a tumor until very recently in the AURORA study²⁹. Our results are consistent with AURORA's observed associations of HER2-mutant samples with the HER2-E subtype and of *ESR1*-mutant samples with the Luminal B subtype in HR+/HER2- MBC.

The association between ER and RTK/MAPK alterations and the PAM50 subtype suggests that some RTK/MAPK oncogenic drivers in HR+/HER2- MBC may induce resistance to endocrine therapy by switching the tumor towards an ER pathway-independent

transcriptional state. In other words, the resistance mechanism class underlying some RTK/MAPK oncogenic drivers might be closer to “Pathway Indifference” than “Pathway Bypass” of the ER pathway^{40,41}. In this view, just as HR + /HER2- BC is endocrine therapy sensitive and most-often in a Luminal A/B transcriptional state and HR-/HER2 + BC is endocrine therapy insensitive and most-often in a HER2-E transcriptional state, certain RTK/MAPK oncogenic drivers might be able push HR + /HER2- MBC tumors to a HER2-E transcriptional state that is endocrine therapy insensitive.

Notably missing from the association between ER and RTK/MAPK mutations were a subset of known RTK/MAPK alterations (*NFI* loss-of-function mutations, *FGFR1* activating mutations and high amplifications). In our case, all samples with these RTK/MAPK alterations also had an activating *ESR1* mutation (Supplementary Fig. 2B) and did not show high activity in RTK pathway signatures (Supplementary Fig. 2A). Co-occurrence of *FGFR1* high amplifications and activating *ESR1* mutations is relatively common (2 cases out of 5 with an *FGFR1* high amplification in our prior study⁵), but co-occurrence *NFI* loss-of-function mutations or *FGFR1* activating mutations and activating *ESR1* mutations are rare (3 cases out of 91 with these *NFI* or *FGFR1* mutations from two recent MSK-IMPACT studies^{9,16}). The observed link between molecular subtype and activating mutations in *ESR1* (Luminal A/B) and *ERBB2/BRAF* (HER2-E) hints at the following possibility for the cases where there are both *ESR1* and RTK/MAPK oncogenic alterations (e.g., in *NFI* and *FGFR1*): *ESR1* mutations drive the tumor towards an ER pathway-dependent transcriptional state that cannot be overcome by RTK/MAPK alterations, resulting in a low RTK pathway signature activity and a Luminal A or B subtype.

We found complexity in the process of acquired resistance to CDK4/6i therapy revealed by tumor evolutionary analysis. Tumor evolutionary analysis of pre- and post-CDK4/6i samples identified acquired genomic alterations in multiple resistance pathways (Figs. 5 and 6). Notable cases include an *ERBB2* amplification in a tumor with a pre-existing *ERBB2*^{L869R} activating mutation, tumors in which the only acquired or enriched alterations were in the ER pathway (*ESR1*^{H524L}, *ESR1*^{D538G}, *GATA3*^{412fs}), and a clonal *BRAF*^{V600E} activating mutation in a tumor with concurrent ER loss (no activating *BRAF* mutations were reported in several previous HR + /HER2- MBC studies^{4,5,11,12,17} and the two reported in Razavi et al.¹⁶ were subclonal). For two patients, we identified co-existing tumor lineages with distinct driver mutations, one dominating the tumor sample and one the ctDNA sample. In one of these patients, each tumor lineage acquired a genomic alteration in *HER2* (*ERBB2* amplification, *ERBB2*^{L755S} mutation), demonstrating convergent evolution of *ERBB2* activation following CDK4/6i therapy (Fig. 5A).

The distinct co-existing tumor lineages from tumor and blood biopsy samples illustrate the complexity of the process of acquired drug resistance across a patient’s tumors. This complexity is particularly evident in the convergent (*ERBB2* activation) and divergent (*ESR1* or *MTOR* activation) paths to resistance identified. Genomic analysis of co-existing tumor lineages provides a unique window into the evolutionary dynamics of tumor drug resistance, and can help identify high-confidence resistance mechanisms, as we did here for *ERBB2* activation and like prior work has done for various targeted therapies^{5,42}. In our work, this was only possible because of the availability of WES for both tumor and blood biopsy samples, and the existence of these distinct co-existing lineages was not uncommon (18%, 2/11 of cases with both sample types). These results highlight the drug resistance insights that can be gained from collecting and analyzing joint tumor and blood biopsy samples.

Our results suggest that mTOR pathway activation is a molecular correlate of response to combined palbociclib, exemestane, and everolimus. Our genomic and transcriptomic analysis of baseline trial samples uncovered hints that clinical benefit to combined ER, CDK4/6, and MTOR inhibition is correlated with activation of the mTOR

pathway (Fig. 7). In particular, we found higher mTORC1 pathway activity and PI3K/AKT/mTOR mutations (including an activating *MTOR* mutation) in clinical benefit-associated samples. We also found that our results were inconclusive in terms of whether *AKT1*^{E17K} mutations are a marker for response to triplet therapy, as one would hypothesize based on everolimus targeting the PI3K/AKT/mTOR pathway. This was because of the four patients with *AKT1*^{E17K} -mutant tumors, two discontinued therapy due to treatment toxicity, while for the remaining cases one derived clinical benefit and one did not.

Our findings that activation of the mTOR pathway correlates with response to triple therapy are only hypothesis-generating, given the limited number of patients that derived clinical benefit. However, they are consistent with recent work by Project GENIE finding a more durable response to everolimus-containing therapy in *AKT1*^{E17K} vs. *AKT1*-wild-type ER + MBC, with the largest effect seen in those patients with *AKT1*^{E17K} and an additional PI3K pathway mutation⁴³. These results stand in contrast with studies of BOLERO-2, which found no association between response to everolimus and alterations in the PI3K/AKT/mTOR pathway, although this difference could be attributed to the shift in treatment landscape due to the approval of fulvestrant and CDK4/6i therapies. More definitive answers could come from comprehensive genomic analyses of other triplet therapy trials like TRINITY-1³⁴, IPATunity150⁴⁴, and others⁴⁵.

Limitations of our study are the modest sample size of our cohort, the limited number of patients with both pre- and post-CDK4/6i tumors, and the lack of a control group with patients with tumors sensitive to CDK4/6i. Another limitation is the inability to distinguish if a candidate driver causes resistance to the endocrine therapy and/or the CDK4/6i component of therapy, given that both therapies are given in combination (a limitation shared with most clinical studies on CDK4/6i).

To conclude, our multi-omics analysis revealed features associated with CDK4/6 inhibitor resistance. These include concurrent *ERBB2* or *BRAF* mutations and a HER2-enriched subtype, and convergent evolution of *ERBB2* activation. Genomic/transcriptomic correlates of response to everolimus-containing triplet therapy hinted at mTOR pathway activation being associated with clinical benefit. These results illustrate how transcriptome sequencing provides complementary and additional information than genome sequencing, and how integrating genomic and transcriptomic data may help better identify patients likely to respond to CDK4/6 inhibitor therapies.

Methods

Some of the methods reported follow closely what has been described in our recent work^{2,5}. For additional details on the methods, refer to the Supplementary Methods.

Compliance with Ethical Standards

The study was conducted in accordance with the International Conference on Harmonization Good Clinical Practice Standards and the Declaration of Helsinki. Institutional review board (IRB) approval was obtained at Dana-Farber/Harvard Cancer Center (DF/HCC). The DF/HCC Data and Safety Monitoring Committee (DSMC), which is composed of clinical specialists with experience in oncology and who had no direct relationship with the study, reviewed and monitored toxicity and accrual data from the study. Information that raised questions or concerns was addressed with the overall PI and study team. Participants provided written informed consent prior to the performance of any protocol specific procedures or assessments.

Patients and samples

Prior to any study procedures, all patients provided written informed consent to participate in the clinical trial and for research biopsies, blood samples, and sequencing of these samples, as approved by the Dana-Farber/Harvard Cancer Center IRB (DF/HCC Protocol 16-177). All

but four patients (patients 7, 26, 36, and 37) additionally co-consented to DF/HCC Protocols 05-246/09-204 and their genomic was included in Supplementary Data 2 and has been deposited in dbGaP (study accession phs001285.v2.p1). Metastatic core biopsies were obtained from patients, and samples were immediately snap-frozen in OCT and stored in -80°C . Archival formalin-fixed, paraffin-embedded (FFPE) blocks of primary tumor samples were also obtained. A blood sample was obtained and whole blood was stored at -80°C . DNA and RNA were extracted from tumors. Germline DNA was extracted from peripheral blood mononuclear cells from whole blood. Cell-free DNA was obtained from plasma for circulating tumor DNA analysis, as described previously⁴⁶. For patient 22, targeted panel sequencing data (Onco-Panel) for two tumors was obtained⁴⁷.

Phase I/II clinical trial

The protocol for the phase I/II clinical trial (NCT02871791) is available at www.clinicaltrials.gov, and includes information related to the study location, eligibility, and compounds. The original protocol is included in Supplementary Data 1, and the latest version of the protocol (DF/HCC Protocol #16-177) is included as a Supplementary Note in the Supplementary Information file.

Study design and patient population. A total of 9 patients were recruited into the phase Ib portion of the study between September 12, 2016 and March 27, 2017, and a total of 32 patients were recruited into the phase IIa portion of the study between May 26, 2017 and June 26, 2019. Eligible participants had histologically or cytologically confirmed HR + /HER2- MBC. Participants enrolled in the phase Ib portion of the study were required to have evaluable disease, whereas participants enrolled in the phase IIa portion were required to have measurable disease per RECIST 1.1⁴⁸. Participants were also required to have radiological or objective evidence of progression on a CDK4/6 inhibitor in the metastatic setting and relapse or progression on a non-steroidal aromatase inhibitor (NSAI) (defined as either relapse within 12 months after completing adjuvant NSAI or progression through a NSAI for metastatic or locally advanced HR+ breast cancer). Any number of prior endocrine therapies were allowed, as long as none were exemestane-based. Up to one prior line of chemotherapy was allowed. Participants were required to be at least 18 years old with an ECOG PS ≤ 2 . In addition, participants enrolled in the phase IIa portion of the study were required to undergo a research biopsy at baseline (before treatment initiation) and at the time of disease progression. Participants were also required to provide a single research blood sample before the initiation of therapy. Participants with demonstrated intolerance to 125 mg palbociclib were ineligible. Additional exclusionary criteria included prior treatment with any mTOR inhibitor or concurrent treatment with other investigational agents.

Procedures. Palbociclib was administered orally, once daily for 21 consecutive days, followed by a 7-day rest (28-day cycle). Everolimus and exemestane were administered orally, once daily for 28 consecutive days (28-day cycle). During phase Ib, participants were treated with increasing/decreasing doses of palbociclib and everolimus to establish the MTD/RP2D for both drugs in the context of the P-E-E combination. The starting dose of palbociclib was 100 mg, which was increased to 125 mg. The starting dose of everolimus was 5 mg, which was increased to 10 mg. Only one of the two study drugs was escalated/de-escalated at a time. If patients developed toxicity to 5 mg everolimus, de-escalation to 2.5 mg was allowed. Palbociclib doses below 100 mg were not explored. Exemestane was maintained at 25 mg. Patients were observed for dose-limiting toxicity (DLT) events, which were defined as adverse events or abnormal laboratory values with a reasonably possible relationship to the study medication(s).

The RP2D for the combination was determined to be palbociclib 100 mg + everolimus 5 mg + exemestane 25 mg²⁰. This dose was used

throughout phase IIa. During phase IIa, patients were evaluated for response every 8 weeks according to RECIST 1.1 criteria⁴⁸. Changes in the largest diameter (unidimensional measurement) of the tumor lesions and the shortest diameter in the case of malignant lymph nodes were used.

Statistical considerations. The primary objective of phase Ib was to determine the safety and tolerability of the combination regimen, and to define the MTD/RP2D. The secondary objectives of this phase were to describe the pharmacokinetics (PK) profile of everolimus and exemestane in the triplet combination and evaluate the potential effect of palbociclib on the PK profile of everolimus. For this portion of the study, participants proceeded in dose escalation following the 3 + 3 rule. Treatment-related toxicities were summarized by maximum grade and by term using CTCAE version 4.0 and reported with 90% binomial exact confidence intervals.

The primary endpoint of phase IIa was to determine the CBR (CR + PR + SD ≥ 24 weeks) of the P-E-E combination. Based on the results of the BOLERO-2 trial⁴⁹, we estimated that the true CBR would be 40%. Thus, we determined that a CBR of $\geq 65\%$ would indicate that the P-E-E regimen is worthy of further study. Recruitment of at least 29 participants would provide 90% power to test the hypothesis (one-sided alpha of 0.1 and type II error of 0.1). In order to account for a 10% drop out rate, a total of 32 participants were recruited over the course of two and a half years. Up to an additional six months of follow-up was required on the last participant accrued to observe response after the final cycle of protocol therapy, for a total study duration of 3 years.

Secondary endpoints included objective response rate (ORR), disease control rate (DCR), duration of response (DOR), and PFS according to investigator assessment. These metrics were reported with 95% confidence intervals.

Clinical annotations

Patient charts were reviewed to determine the sequence of treatments received in the neoadjuvant, adjuvant, and metastatic setting, the treatments' dates and durations, and the dates of the available biopsy samples. The dates and duration of the prior CDK4/6 inhibitor treatment was obtained for all patients for which exome or transcriptome sequencing passed quality control in at least one sample. The dates and duration of the complete sequence of treatments up until discontinuation of the clinical trial regime were obtained for selected patients with 2 or more tumor or cfDNA samples (Figs. 5 and 6).

Biopsy phenotypes to prior CDK4/6i response

A phenotype of response to the prior CDK4/6i treatment was assigned to each baseline tumor or cfDNA samples following⁵, and using duration of treatment as a proxy for treatment response. All baseline samples for which sequencing data passed quality control were taken after progression on the prior CDK4/6 inhibitor. Thus, these post-CDK4/6i samples were assigned an acquired resistance phenotype if time on the prior CDK4/6i treatment was >6 months and an intrinsic resistance phenotype otherwise. The resistance phenotype, prior CDK4/6i treatment duration, and drugs received as part of the prior CDK4/6i treatment can be found in Supplementary Data 6.

Whole exome sequence data processing and analysis

Data processing and quality control. Whole exome sequences for each tissue/blood sample were captured using Illumina technology and the sequencing data processing and analysis was performed using the Picard and Terra pipelines at the Broad Institute. The Picard pipeline (<http://picard.sourceforge.net>) was used to produce a BAM file with aligned reads. This includes alignment to the GRCh37 human reference sequence using the BWA aligner⁵⁰ and estimation and recalibration of base quality score with the Genome Analysis Toolkit (GATK)⁵¹.

A custom-made cancer genomics analysis pipeline was used to identify somatic alterations using the Terra platform (<https://app.terra.bio/>). The CGA WES Characterization pipeline developed at the Broad Institute was used to call, filter and annotate somatic mutations and copy number variation. See Supplementary Methods for details of the variant calling pipeline used in this study. GATK CNV⁵² was used for the generation of accurate relative copy-number profiles from the whole exome sequencing data and reference/alternate read counts at heterozygous SNP sites present in both the normal and tumor samples. After accurate proportional coverage profiles are generated for a sample, Allelic CapSeg tool⁵³ was used to generate a segmented allelic copy ratio profile. Allelic copy number profile and mutational call data were modeled jointly by ABSOLUTE⁵⁴ to produce purity for the samples, a discrete copy number profile, and compute cancer cell fractions (CCF). Tumor samples which had a purity of 8% or more were used for downstream analysis.

Annotating oncogenic mutations. OncoKB⁵⁵ was used to annotate known oncogenic mutations, identify their effect (e.g., loss or gain of function) and if they are known cancer hotspots.

Tumor evolutionary analysis. Patients with >1 tumor or cfDNA WES samples collected from different timepoints/locations were used to study tumor evolution and tumor heterogeneity. To properly compare SNVs and indels in samples from the same patient, the union of all mutations called in each patient's samples were considered. The reference and alternate reads in each patient's samples were used as input for ABSOLUTE⁵⁴ to compute cancer cell fractions. The clonal structure and the evolutionary history of the clones (phylogenetic tree) was inferred with PhylogicNDT⁵⁶ using only SNV sites and retaining only clones with at least four mutations and cancer cell fraction of more than 1%.

Corrected quantification of copy number, gene deletions, and biallelic inactivations. The inference of gene amplifications, gene deletions, and biallelic inactivations were based on the copy number profile obtained from ABSOLUTE⁵⁴. To infer biallelic inactivations, mutational events that included both loss of heterozygosity (LOH) and a loss-of-function mutation (LOF) (loss-of-function or likely loss-of-function OncoKB-annotated mutation, or a Nonsense Mutation, Nonstop_Mutation, Frame_Shift_Del, or Frame_Shift_Del mutation) were used. Gene amplifications and deep deletions were based on the purity corrected measure for the segment containing that gene. Genes in a segment-specific copy number of less than 0.5 were considered deep deletions (Deep DEL). To measure segment-specific copy number amplifications, the genome ploidy was subtracted for each sample to obtain the copy number above ploidy (CNAP). CNAPs of at least 3 are considered as amplifications (AMP); CNAPs above 1.5, but below 3 are considered low amplification (GAIN); CNAPs of at least 6 are considered high amplifications (High AMP), and CNAPs of at least 9 and no more than 100 genes are considered focal high amplification (Focal High AMP). In the figures, AMP or GAIN copy number amplifications were not included for any sample and Deep DELs were not included for cfDNA samples (because of limited concordance between tumor and cfDNA Deep DELs, unlike most other alterations).

Statistical tests and analysis

Statistical significance of the association between signature activities and oncogenic mutations was measured using a one-sided Mann-Whitney test, and is based on whether the AUC ROC score outperforms a random classifier⁵⁷. Statistical significance of the association between the Hallmark signature scores in baseline tumors and clinical benefit was measured using a two-sided Welch's *t*-test. Statistical significance of the enrichment of upper or lower quartile Hallmark signature scores in the baseline tumors of patients that derived clinical benefit was measured using a two-sided Fisher exact test. A $P < 0.05$

was considered to be statistically significant. All statistical analysis was performed using R (version 4.0.3).

Transcriptome sequencing data processing and analysis

Data processing and quality control. RNA-seq reads were mapped to the human genome (hg19) with STAR aligner⁵⁸ with default parameters. Transcriptome quality was assessed using RNA-SeQC 2⁵⁹ and expression quantification was conducted using RSEM⁶⁰. Samples with <8000 unique genes were removed from subsequent analysis. Gene expression was measured using $\log_2(\text{TPM} + 1)$ values and corrected for tissue type (frozen vs. FFPE) using ComBat⁶¹. The exception was the analysis in Fig. 7B, C, in which only baseline (T1) samples from frozen tissue were considered, and uncorrected $\log_2(\text{TPM} + 1)$ values were used. Figure 7D used the same set of samples as Fig. 7B, C.

Transcriptional signature activity. To calculate the activity of a transcriptional signature or gene set, we used single-sample gene set enrichment analysis (ssGSEA). ssGSEA was performed for all tumor samples using fgsea⁶² to calculate normalized enrichment scores for Hallmark gene sets from the Molecular Signatures Database⁶³ using upper quartile normalized expression values PAM50 molecular subtype assignment. To assign research-based PAM50 subtypes, expression values were rescaled relative to those of a receptor status-balanced Metastatic Breast Cancer Project (MBCProject) cohort, in which samples were re-sampled to achieve the ER-positive to ER-negative receptor status ratio in the UNC training set, from which the PAM50 subtype centroids were derived^{27,64}. genefu was used to call research-based PAM50 subtypes⁶⁵ using the rescaled expression values and spearman correlation to the PAM50 subtype centroids. Samples with a PAM50 centroid correlation <0.10 for each centroid were not assigned a PAM50 subtype (Not Classified, NC).

Relative gene expression and transcriptional signature activity. To calculate the quantiles for gene expression and transcriptional signature activity, the receptor status-balanced MBCProject cohort was used as a reference cohort. Upper quartile normalized expression was used for relative gene expression and ssGSEA normalized enrichment scores calculated from upper quartile normalized expression was used for relative transcriptional signature activity.

Reporting summary

Further information on research design is available in the Nature Portfolio Reporting Summary linked to this article.

Data availability

Tumor and germline whole-exome sequencing data and RNA sequencing data generated and analyzed for this study have been deposited in the database of Genotypes and Phenotypes (dbGaP) under study accession phs001285.v2.p1 [https://www.ncbi.nlm.nih.gov/projects/gap/cgi-bin/study.cgi?study_id=phs001285.v1.p1]. These data are available under controlled access to protect individual's privacy. Access can be requested through dbGaP and use restrictions are specified by the Health/Medical/Biomedical and Disease-Specific (Breast Cancer) consent groups. Processed de-identified data generated in this study including clinical trial protocol and data, patient metadata, and tumor exome and transcriptome analysis are available in Supplementary Data 1–8. Four patients (patients 7, 26, 36, and 37) did not co-consent to the additional DF/HCC Protocols 05-246/09-204, and their genomic data is not included in Supplementary Data 2 and was not deposited in dbGaP. Requests for additional raw and processed data and materials will be reviewed by the senior authors to determine whether the request is subject to any intellectual property or confidentiality obligations. These additional data and materials may be subject to patient confidentiality and might require a material transfer agreement. The remaining data are available within the Article, Supplementary Information or Source Data file. Source data are provided as a Source Data file. Source data are provided with this paper.

Code availability

All software and pipelines for genomic data generation are described in detail in the Methods and the Supplementary Methods. The scripts used to generate the figures are available upon request from the corresponding author.

References

- Spring, L. M. et al. Cyclin-dependent kinase 4 and 6 inhibitors for hormone receptor-positive breast cancer: past, present, and future. *Lancet* **395**, 817–827 (2020).
- Condorelli, R. et al. Polyclonal RB1 mutations and acquired resistance to CDK 4/6 inhibitors in patients with metastatic breast cancer. *Ann. Oncol.* **29**, 640–645 (2018).
- O’Leary, B. et al. The genetic landscape and clonal evolution of breast cancer resistance to palbociclib plus fulvestrant in the PALOMA-3 trial. *Cancer Discov.* **8**, 1390–1403 (2018).
- Li, Z. et al. Loss of the FAT1 tumor suppressor promotes resistance to CDK4/6 inhibitors via the hippo pathway. *Cancer Cell* **34**, 893–905.e898 (2018).
- Wander, S. A. et al. The genomic landscape of intrinsic and acquired resistance to cyclin-dependent kinase 4/6 inhibitors in patients with hormone receptor-positive metastatic breast cancer. *Cancer Discov.* **10**, 1174–1193 (2020).
- Turner, N. C. et al. Cyclin E1 expression and palbociclib efficacy in previously treated hormone receptor-positive metastatic breast cancer. *J. Clin. Oncol.* **37**, 1169–1178 (2019).
- Yang, C. et al. Acquired CDK6 amplification promotes breast cancer resistance to CDK4/6 inhibitors and loss of ER signaling and dependence. *Oncogene* **36**, 2255–2264 (2017).
- Cornell, L., Wander, S. A., Visal, T., Wagle, N. & Shapiro, G. I. MicroRNA-mediated suppression of the TGF-beta pathway confers transmissible and reversible CDK4/6 inhibitor resistance. *Cell Rep.* **26**, 2667–2680.e2667 (2019).
- Li, Q. et al. INK4 tumor suppressor proteins mediate resistance to CDK4/6 kinase inhibitors. *Cancer Discov.* **12**, 356–371 (2022).
- Prat, A. et al. Correlative biomarker analysis of intrinsic subtypes and efficacy across the MONALEESA phase III studies. *J. Clin. Oncol.* **39**, 1458–1467 (2021).
- Nayar, U. et al. Acquired HER2 mutations in ER(+) metastatic breast cancer confer resistance to estrogen receptor-directed therapies. *Nat. Genet.* **51**, 207–216 (2019).
- Mao, P. et al. Acquired FGFR and FGF alterations confer resistance to estrogen receptor (ER) targeted therapy in ER(+) metastatic breast cancer. *Clin. Cancer Res.* **26**, 5974–5989 (2020).
- Costa, C. et al. PTEN loss mediates clinical cross-resistance to CDK4/6 and PI3Kalpha inhibitors in breast cancer. *Cancer Discov.* **10**, 72–85 (2020).
- Formisano, L. et al. Aberrant FGFR signaling mediates resistance to CDK4/6 inhibitors in ER+ breast cancer. *Nat. Commun.* **10**, 1373 (2019).
- Turner, N. et al. FGFR1 amplification drives endocrine therapy resistance and is a therapeutic target in breast cancer. *Cancer Res.* **70**, 2085–2094 (2010).
- Razavi, P. et al. The genomic landscape of endocrine-resistant advanced breast cancers. *Cancer Cell* **34**, 427–438.e426 (2018).
- Bertucci, F. et al. Genomic characterization of metastatic breast cancers. *Nature* **569**, 560–564 (2019).
- Hanker, A. B., Sudhan, D. R. & Arteaga, C. L. Overcoming endocrine resistance in breast cancer. *Cancer Cell* **37**, 496–513 (2020).
- Baselga, J. et al. Everolimus in postmenopausal hormone-receptor-positive advanced breast cancer. *N. Engl. J. Med.* **366**, 520–529 (2012).
- Barroso-Sousa, R. et al. A phase I study of palbociclib (PALBO) plus everolimus (EVE) and exemestane (EXE) in hormone-receptor positive (HR+)/HER2- metastatic breast cancer (MBC) after progression on a CDK4/6 inhibitor (CDK4/6i): safety, tolerability and pharmacokinetic (PK) analysis. *J. Clin. Oncol.* **36**, 1068–1068 (2018).
- Grabiner, B. C. et al. A diverse array of cancer-associated MTOR mutations are hyperactivating and can predict rapamycin sensitivity. *Cancer Discov.* **4**, 554–563 (2014).
- Wagle, N. et al. Activating mTOR mutations in a patient with an extraordinary response on a phase I trial of everolimus and pazopanib. *Cancer Discov.* **4**, 546–553 (2014).
- Kwiatkowski, D. J. et al. Mutations in TSC1, TSC2, and MTOR are associated with response to rapalogs in patients with metastatic renal cell carcinoma. *Clin. Cancer Res.* **22**, 2445–2452 (2016).
- Xu, J. et al. Mechanistically distinct cancer-associated mTOR activation clusters predict sensitivity to rapamycin. *J. Clin. Invest.* **126**, 3526–3540 (2016).
- Hyman, D. M. et al. HER kinase inhibition in patients with HER2- and HER3-mutant cancers. *Nature* **554**, 189–194 (2018).
- Bose, R. et al. Activating HER2 mutations in HER2 gene amplification negative breast cancer. *Cancer Discov.* **3**, 224–237 (2013).
- Prat, A. & Parker, J. S. Standardized versus research-based PAM50 intrinsic subtyping of breast cancer. *Clin. Transl. Oncol.* **22**, 953–955 (2020).
- Wagle, N. et al. The Metastatic Breast Cancer Project: a national direct-to-patient initiative to accelerate genomics research. *J. Clin. Oncol.* **34**, LBA1519 (2016).
- Aftimos, P. et al. Genomic and transcriptomic analyses of breast cancer primaries and matched metastases in AURORA, the breast international group (BIG) molecular screening initiative. *Cancer Discov.* **11**, 2796–2811 (2021).
- Sanchez-Guixe, M. et al. High FGFR1-4 mRNA expression levels correlate with response to selective FGFR inhibitors in breast cancer. *Clin. Cancer Res.* **28**, 137–149 (2022).
- Wander, S. A. et al. Abstract PD7-08: Igf1r mediates cdk4/6 inhibitor (cdk4/6i) resistance in tumor samples and in cellular models. *Cancer Res.* **81**, PD7-08-PD07-08 (2021).
- Fox, E. M. et al. A kinome-wide screen identifies the insulin/IGF-I receptor pathway as a mechanism of escape from hormone dependence in breast cancer. *Cancer Res.* **71**, 6773–6784 (2011).
- Hurvitz, S. A. et al. Abstract PD13-03: Ribociclib, everolimus, exemestane triplet therapy in HR+/HER2- advanced breast cancer after progression on a CDK4/6 inhibitor: final efficacy, safety, and biomarker results from TRINITY-1. *Cancer Res.* **82**, PD13-03-PD13-03 (2022).
- Bardia, A. et al. Phase I/II trial of exemestane, ribociclib, and everolimus in women with HR(+)/HER2(-) advanced breast cancer after progression on CDK4/6 inhibitors (TRINITY-1). *Clin. Cancer Res.* **27**, 4177–4185 (2021).
- Bidard, F. C. et al. Elacestrant (oral selective estrogen receptor degrader) Versus Standard Endocrine Therapy for Estrogen Receptor-Positive, Human Epidermal Growth Factor Receptor 2-Negative Advanced Breast Cancer: Results From the Randomized Phase III EMERALD Trial. *J. Clin. Oncol.* **40**, 3246–3256 (2022).
- Wander, S. A. et al. Clinical outcomes with abemaciclib after prior CDK4/6 inhibitor progression in breast cancer: A multicenter experience. *J. Natl. Compr. Canc Netw.* 1–8 <https://doi.org/10.6004/jnccn.2020.7662> (2021).
- Kalinsky, K. et al. A randomized, phase II trial of fulvestrant or exemestane with or without ribociclib after progression on anti-estrogen therapy plus cyclin-dependent kinase 4/6 inhibition (CDK 4/6i) in patients (pts) with unresectable or hormone receptor-positive (HR+), HER2-negative metastatic breast cancer (MBC): MAINTAIN trial. *J. Clin. Oncol.* **40**, LBA1004 (2022).
- Freeman-Cook, K. et al. Expanding control of the tumor cell cycle with a CDK2/4/6 inhibitor. *Cancer Cell* **39**, 1404–1421.e1411 (2021).
- Hafner, M. et al. Multiomics profiling establishes the polypharmacology of FDA-approved CDK4/6 inhibitors and the

- potential for differential clinical activity. *Cell Chem. Biol.* **26**, 1067–1080.e1068 (2019).
40. Konieczkowski, D. J., Johannessen, C. M. & Garraway, L. A. A convergence-based framework for cancer drug resistance. *Cancer Cell* **33**, 801–815 (2018).
 41. Vasan, N., Baselga, J. & Hyman, D. M. A view on drug resistance in cancer. *Nature* **575**, 299–309 (2019).
 42. Juric, D. et al. Convergent loss of PTEN leads to clinical resistance to a PI(3)Kalpha inhibitor. *Nature* **518**, 240–244 (2015).
 43. Smyth, L. M. et al. Characteristics and outcome of AKT1 (E17K)-mutant breast cancer defined through AACR project GENIE, a clinicogenomic registry. *Cancer Discov.* **10**, 526–535 (2020).
 44. Oliveira, M. et al. Abstract P5-16-11: Ipatasertib (ipat) in combination with palbociclib (palbo) and fulvestrant (fulv) in patients (pts) with hormone receptor-positive (HR+) HER2-negative advanced breast cancer (aBC). *Cancer Res.* **82**, P5-16-11–P15-16-11 (2022).
 45. Layman, R. et al. Abstract PD13-02: phase Ib expansion study of gedatolisib in combination with palbociclib and endocrine therapy in women with ER+ metastatic breast cancer. *Cancer Res.* **82**, PD13-02–PD13-02 (2022).
 46. Adalsteinsson, V. A. et al. Scalable whole-exome sequencing of cell-free DNA reveals high concordance with metastatic tumors. *Nat. Commun.* **8**, 1324 (2017).
 47. Garcia, E. P. et al. Validation of OncoPanel: a targeted next-generation sequencing assay for the detection of somatic variants in cancer. *Arch. Pathol. Lab. Med.* **141**, 751–758 (2017).
 48. Eisenhauer, E. A. et al. New response evaluation criteria in solid tumours: revised RECIST guideline (version 1.1). *Eur. J. Cancer* **45**, 228–247 (2009).
 49. Beaver, J. A. & Park, B. H. The BOLERO-2 trial: the addition of everolimus to exemestane in the treatment of postmenopausal hormone receptor-positive advanced breast cancer. *Future Oncol.* **8**, 651–657 (2012).
 50. Li, H. & Durbin, R. Fast and accurate short read alignment with Burrows-Wheeler transform. *Bioinformatics* **25**, 1754–1760 (2009).
 51. McKenna, A. et al. The Genome Analysis Toolkit: a MapReduce framework for analyzing next-generation DNA sequencing data. *Genome Res.* **20**, 1297–1303 (2010).
 52. Van der Auwera GAaOC, B. D. *Genomics in the Cloud: Using Docker, GATK, and WDL in Terra 1st Edition*. O'Reilly Media, Inc. (2020).
 53. Landau, D. A. et al. Evolution and impact of subclonal mutations in chronic lymphocytic leukemia. *Cell* **152**, 714–726 (2013).
 54. Carter, S. L. et al. Absolute quantification of somatic DNA alterations in human cancer. *Nat. Biotechnol.* **30**, 413–421 (2012).
 55. Chakravarty, D. et al. OncoKB: a precision oncology knowledge base. *JCO Precis. Oncol.* **2017** 1–16 (2017).
 56. Leshchiner, I., et al. Comprehensive analysis of tumour initiation, spatial and temporal progression under multiple lines of treatment. *bioRxiv*, 508127 (2019).
 57. Mason, S. J. & Graham, N. E. Areas beneath the relative operating characteristics (ROC) and relative operating levels (ROL) curves: Statistical significance and interpretation. *Quart. J. R. Meteorol. Soc.* **128**, 2145–2166 (2002).
 58. Dobin, A. et al. STAR: ultrafast universal RNA-seq aligner. *Bioinformatics* **29**, 15–21 (2013).
 59. Graubert, A., Aguet, F., Ravi, A., Ardlie, K. G., Getz, G. RNA-SeqQC 2: efficient RNA-seq quality control and quantification for large cohorts. *Bioinformatics* **37**, 3048–3050 (2021).
 60. Li, B. & Dewey, C. N. RSEM: accurate transcript quantification from RNA-Seq data with or without a reference genome. *BMC Bioinform.* **12**, 323 (2011).
 61. Leek, J. T., Johnson, W. E., Parker, H. S., Jaffe, A. E. & Storey, J. D. The sva package for removing batch effects and other unwanted variation in high-throughput experiments. *Bioinformatics* **28**, 882–883 (2012).
 62. Korotkevich, G. et al. Fast gene set enrichment analysis. *bioRxiv*, 060012 (2021).
 63. Liberzon, A. et al. The Molecular Signatures Database (MSigDB) hallmark gene set collection. *Cell Syst.* **1**, 417–425 (2015).
 64. Parker, J. S. et al. Supervised risk predictor of breast cancer based on intrinsic subtypes. *J. Clin. Oncol.* **27**, 1160–1167 (2009).
 65. Gendoo, D. M. et al. Genefu: an R/Bioconductor package for computation of gene expression-based signatures in breast cancer. *Bioinformatics* **32**, 1097–1099 (2016).

Acknowledgements

We thank all the patients who participated in the clinical trial and provided the samples analyzed in this work, without whom this work would not have been possible. This work was supported by an ASPIRE grant from Pfizer (to S. Tolaney), Saverin Breast Cancer Research Fund (to Dana-Farber/Harvard Cancer Center), NCI Specialized Program of Research Excellence (SPORE) Grant 1P50CA168504 (to Dana-Farber/Harvard Cancer Center), Susan G. Komen CCR15333343 (to N. Wagle), The Breast Cancer Alliance (to N. Wagle), The Cancer Couch Foundation (to N. Wagle), and Twisted Pink (to N. Wagle). The sponsors did not participate in the study's design or research.

Author contributions

Study conduct and design: J.G., R.B.-S., A.H.P., B.O., N.U.L., N.T., S.T., and N.W. Specimen collection: A.P., E.W., K.H., and M.H. Data acquisition: A.P., E.W., D.L.A., K.H., and M.H. Statistical analysis: Q.J., T.L., and N.T. Data interpretation: J.G., R.B.-S., A.F., D.L.A., E.J., J.E.B.-B., Q.J., T.L., S.T., and N.W. Drafting the manuscript or revising it critically: J.G., R.B.-S., Q.J., N.T., A.H.P., B.O., N.U.L., S.T., and N.W. Final approval of the manuscript: J.G., R.B.-S., S.T., and N.W.

Competing interests

J.G. owns stocks in the biotechnology exchange-traded funds CNCR, IDNA, IBB, and XBI, and owned stocks in Adaptive Biotechnologies, 2seventy bio, and bluebird bio. R.B.-S. has received consulting fees from AstraZeneca, Eli Lilly, Libbs, Merck, Roche, and Zodiac; non-CME fees from Bard Access, BMS, Eli Lilly, Libbs, Merck, Novartis, Pfizer, and Roche; has carried out contracted research for Roche; and has received travel, accommodation and expenses from Eli Lilly, Roche, Daiichi Sankyo, and Merck. E.J. is a current employee of Repare Therapeutics. J.E.B.-B. is a current employee of Cellarity. A.R.F. has received honoraria from Bayer, Daiichi Sankyo, Novartis, and Roche; and has received travel grants from Roche. N.U.L. has received consulting fees from Puma, Seattle Genetics, Daichii-Sankyo, AstraZeneca, Denali Therapeutics, Prelude Therapeutics, Olema Pharmaceuticals, Aleta BioPharma, Affinia Therapeutics, Voyager Therapeutics, Janssen, and Blueprint Medicines; has received institutional research support from Genentech, Pfizer, Merck, Seattle Genetics, Zion Pharmaceuticals, Olema Pharmaceuticals, and AstraZeneca; and has stocks and other ownership interests in Artera Inc. (<\$50k and <5% as it relates to consulting activities—options are not currently valued or in-hand); and royalties from UptoDate (book). N.W. is a current employee of Genentech; has been a consultant/advisor for Eli Lilly; has been in the scientific advisory board for Relay Therapeutics and Flare Therapeutics; has received grant support from AstraZeneca and Puma Biotechnologies. S.M.T. reports consulting or advisory roles for Novartis, Pfizer, Merck, Eli Lilly, AstraZeneca, Genentech/Roche, Eisai, Sanofi, Bristol Myers Squibb, Seattle Genetics, CytomX Therapeutics, Daiichi Sankyo, Gilead, Ellipses Pharma, 4D Pharma, OncoSec Medical Inc., BeyondSpring Pharmaceuticals, OncXerna, Zymeworks, Zentalis, Blueprint Medicines, Reveal Genomics, ARC Therapeutics, Infinity Therapeutics, Myovant, Zetagen, Umoja Biopharma, Artios Pharma, Menarini/Stemline, Aadi Biopharma, Bayer, and Incyte Corp; and research funding from Genentech/Roche, Merck, Exelixis, Pfizer, Novartis, Bristol Myers Squibb, Eisai, AstraZeneca, Gilead, NanoString Technologies, Gilead, Seattle Genetics, and OncoPep. The remaining authors declare no competing interests.

Additional information

Supplementary information The online version contains supplementary material available at <https://doi.org/10.1038/s41467-024-45835-6>.

Correspondence and requests for materials should be addressed to Nikhil Wagle.



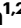


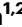


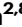


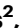


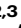




Peer review information *Nature Communications* thanks Jairam Krishnamurthy and the other, anonymous, reviewer(s) for their contribution to the peer review of this work.

Reprints and permissions information is available at <http://www.nature.com/reprints>

Publisher's note Springer Nature remains neutral with regard to jurisdictional claims in published maps and institutional affiliations.

Open Access This article is licensed under a Creative Commons Attribution 4.0 International License, which permits use, sharing, adaptation, distribution and reproduction in any medium or format, as long as you give appropriate credit to the original author(s) and the source, provide a link to the Creative Commons licence, and indicate if changes were made. The images or other third party material in this article are included in the article's Creative Commons licence, unless indicated otherwise in a credit line to the material. If material is not included in the article's Creative Commons licence and your intended use is not permitted by statutory regulation or exceeds the permitted use, you will need to obtain permission directly from the copyright holder. To view a copy of this licence, visit <http://creativecommons.org/licenses/by/4.0/>.

© The Author(s) 2024

Jorge Gómez Tejeda Zañudo ^{1,2,3,10}, **Romualdo Barroso-Sousa** ^{2,3,4,10}, **Esha Jain** ^{1,2,6}, **Qingchun Jin** ⁵, **Tianyu Li** ⁵, **Jorge E. Buendia-Buendia** ^{1,2,7}, **Alyssa Pereslete** ², **Daniel L. Abravanel** ^{1,2,3}, **Arlindo R. Ferreira** ^{2,8}, **Eileen Wrabel** ², **Karla Helvie** ², **Melissa E. Hughes** ², **Ann H. Partridge** ^{2,3}, **Beth Overmoyer** ^{2,3}, **Nancy U. Lin** ^{2,3}, **Nabihah Tayob** ^{2,3,5}, **Sara M. Tolaney** ^{2,3,11} & **Nikhil Wagle** ^{1,2,3,9,11} 

¹Cancer Program, Eli and Edythe L. Broad Institute of MIT and Harvard, Cambridge, MA, USA. ²Medical Oncology, Dana-Farber Cancer Institute, Boston, MA, USA. ³Department of Medicine, Harvard Medical School, Boston, MA, USA. ⁴Oncology Center, Hospital Sírio-Libanês, Brasília, Brazil. ⁵Department of Data Science, Dana-Farber Cancer Institute, Boston, Massachusetts, MA, USA. ⁶Present address: Repare Therapeutics, Cambridge, MA, USA. ⁷Present address: Cellarity, Somerville, MA, USA. ⁸Present address: Breast Unit, Champalimaud Clinical Centre, Champalimaud Foundation, Lisbon, Portugal. ⁹Present address: Genentech, South San Francisco, CA, USA. ¹⁰These authors contributed equally: Jorge Gómez Tejeda Zañudo, Romualdo Barroso-Sousa.

¹¹These authors jointly supervised this work: Sara M. Tolaney, Nikhil Wagle. ✉ e-mail: Nikhil_Wagle@dfci.harvard.edu